ERCB/AGS Open File Report 2012-03

Turtle Mountain Field Laboratory, Alberta (NTS 82G): 2010 Data and Activity Summary

Energy Resources Conservation Board

Alberta Geological Survey

ERCB/AGS Open File Report 2012-03

Turtle Mountain Field Laboratory, Alberta (NTS 82G): 2010 Data and Activity Summary

F. Moreno and C.R. Froese

Energy Resources Conservation Board
Alberta Geological Survey

March 2012

ISBN 978-1-4601-0075-2

If you use information from this publication in other publications or presentations, please give due acknowledgement to ERCB/AGS. We recommend the following reference format:

Moreno, F. and Froese, C.R. (2012): Turtle Mountain Field Laboratory, Alberta (NTS 82G): 2010 data and activity summary; Energy Resources Conservation Board, ERCB/AGS Open File Report 2011-03, 32 p.

Published March 2012 by
Energy Resources Conservation Board
Alberta Geological Survey
4th Floor, Twin Atria Building
4999 – 98th Avenue
Edmonton, Alberta T6B 2X3
Canada

Tel: 780.422.1927
Fax: 780.422.1918
E-mail: AGS-Info@ercb.ca
Website: www.ags.gov.ab.ca

Contents

Tables

Figures

Acknowledgements

The authors acknowledge the following colleagues and collaborators who have contributed either to the operation and maintenance of the Turtle Mountain monitoring system or to studies on the mountain during 2010:

- J. Dehls, J. Warren and J. Morgan (Alberta Geological Survey, Energy Resources Conservation Board)
- D. Walker (Technology Support and Infrastructure, Energy Resources Conservation Board)
- A. Pedrazzini, M. Jaboyedoff, F. Humair and M. Charrière (University of Lausanne, Lausanne, Switzerland)
- H. Bland (Pinnacle Technologies, Calgary, Alberta)
- G. Bjorgan (NavStar Geomatics Ltd., Kelowna, British Columbia)
- B. Teskey and A. Eberling (University of Calgary, Calgary, Alberta)

Abstract

Since 2005, Turtle Mountain has been the site of ongoing monitoring and research focused on understanding the structure and kinematics of movements of the unstable eastern slopes. As this site provides a rich dataset and optimal conditions for the application of new and evolving warning and characterization technologies, the site has been termed the ‘Turtle Mountain Field Laboratory’ (TMFL). This report provides a summary of both the results and the lessons learned from the Turtle Mountain Monitoring System (TMMS) and from studies undertaken by the Alberta Geological Survey (AGS) and collaborators between January 1 and December 31, 2010.

The Turtle Mountain Monitoring System (TMMS) is a near–real-time monitoring system that provides data from a network of more than 80 geotechnical sensors on the South Peak of Turtle Mountain in the Crowsnest Pass of southwestern Alberta. Beginning April 1, 2005, the Energy Resources Conservation Board (ERCB), through the Alberta Geological Survey (AGS), took sole ownership of this system and the responsibility for long-term monitoring, interpretation of data and notification of the Alberta Emergency Management Agency (AEMA) should significant movements occur.

As part of this responsibility, AGS performs an annual detailed review of the data stream. To help in this interpretation, AGS initiated specific studies to understand better the structure of the mountain and its relationship to the style and rate of movement seen in recent and historical deformations of South Peak. These studies also define better the unstable volumes in the South Peak and Third Peak areas.

This report comprises four sections. Section 1 contains information about the major changes to the physical-sensor network of the monitoring system during the summer of 2009. This includes a review of the repair and maintenance activities, a summary of new installations and a summary of system performance and reliability.

Section 2 provides interpretations of slope conditions and displacement behaviour from instrumentation results. Since climatic factors have affected some of the sensors, this discussion focuses only on the sensors that have provided reliable annual data. Meteorological data receive special attention because they have been essential in explaining general displacement trends observed in the surface instrumentation. In general, near–real-time data continue to show trends related both to seasonal thermal cycles and to slow, long-term creep of the South Peak mass. The observed trends highlight very slow movement along the deep fractures on the west side of South Peak, approximately less than a millimetre per year.

Section 3 focuses on the most recent studies, including 1) results of the field study of the Frank Slide debris, and 2) an update on the displacement trends revealed by a series of eighteen points established as part of a periodic GPS monitoring system.

From a risk-management perspective, the ERCB and provincial and municipal emergency-response officials still consider that a single large failure event is the basis for planning of evacuations and road closures. Sensor networks installed by AGS and contractors during the past three years continue to be used to distinguish between the zones of movement and to define scenarios where failure could occur incrementally rather than in a single event.

1 Introduction

In 2005, Alberta Geological Survey (AGS) assumed responsibility for the long-term monitoring and studying of a large, slowly moving rock slide at Turtle Mountain (Figure 1). The first priority for monitoring and studying Turtle Mountain is to provide an early warning to residents in the event of a catastrophic rock avalanche originating from South Peak. The secondary priority is to provide an opportunity for the research community to test and develop instrumentation and monitoring technologies, and to better understand the mechanics of slowly moving rock masses, hence the working name 'Turtle Mountain Field Laboratory' (TMFL). The ERCB/AGS will make available to the research community all data from the TMFL, which will enable researchers to test and develop new monitoring technologies on the mountain. This ongoing research will aid in understanding the movements of the entire South Peak mass, including the lower slope, thereby providing a better model for prediction of future movements. For information on recent developments with the TMFL, please visit the Alberta Geological Survey website at http://www.ags.gov.ab.ca/geohazards/turtle_mountain/turtle_mountain.html.

This yearly report provides the public and researchers with a synthesized update on data trends and research on the mountain as a stimulus for further research. This report is a brief overview and, in many cases, refers to other papers/articles that provide additional detail regarding the information provided here.

2 Sensor Network Activity

This section provides an overview of the major upgrades, repair and maintenance activities on the monitoring system during 2010. A detailed description of the elements that make up this system is available in the 2005 and 2006 data and activity summary reports (Moreno and Froese, 2006, 2008a) and is therefore not included in this summary. Modifications to the system prior to 2010 are fully documented in subsequent summary reports (Moreno and Froese, 2008b, 2009, 2011).

The main activities undertaken with respect to the sensor network during 2010 included (Bjorgan, 2010; Laffin, 2010)

- restoration of wireless communication with the borehole and weather stations;
- upgrade of weather-station elements;
- upgrade of the power-supply system at the different continuous-reading differential GPS (dGPS) stations;
- replacement of damaged dGPS sensors due to the lightning event of September 2009; and
- repair of the primary radio link for the existing continuous-reading dGPS monitoring network.

The following subsections provide a brief overview and photographs of these activities. Figure 2 is an overview of the sensor-network layout as of December 2010.

2.1 New Installations

2.1.1 Replacement of Radio Link for Borehole and Weather Stations

The borehole and weather stations are the datalogging sites for the primary sensor network of the monitoring system. Data recorded at these locations are relayed to the Provincial Building at Blairmore via a radio link and then transferred to ERCB offices in Calgary via an Internet connection. All data received at the ERCB offices are then written to an SQL database.

The radio link operated well for several years until the end of 2009, when the system started to show some signs of deterioration. Several temporary outages occurred during this period, until the radio link ceased operating in January 2010. After some testing, it was clear the radio-link signal was being drowned by other radio sources, most likely a nearby cellular communication tower built recently in Blairmore. Since a radio connection was no longer possible, it was decided to switch to cellular modems. Two cellular modems were purchased, activated and tested on the ground, and installed successfully at the borehole and weather stations (Figure 3). To lower power consumption of the system, the modems are programmed to be on for only a few minutes each hour to send recorded data.

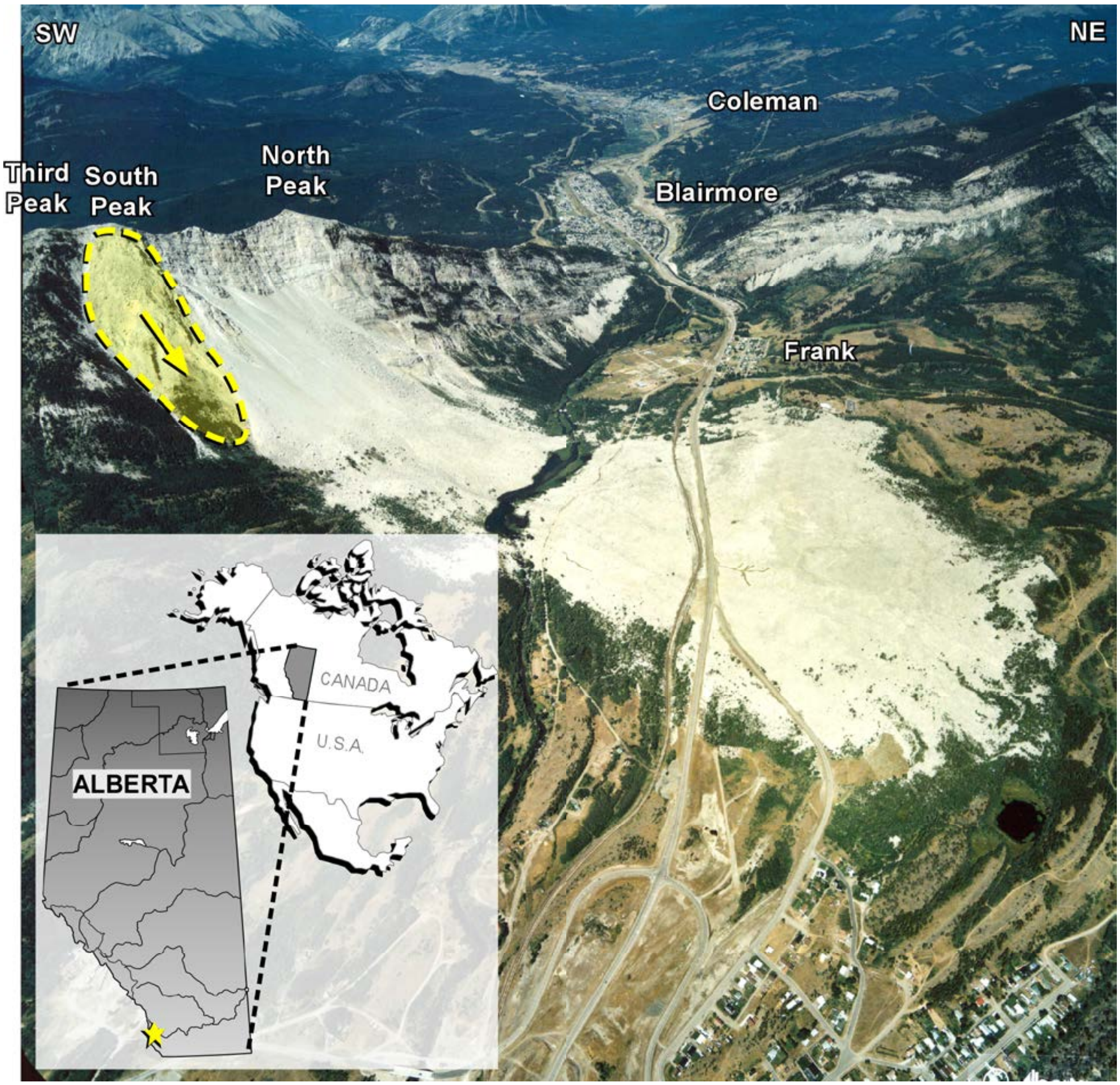

Figure 1. Location of Turtle Mountain in southwestern Alberta and full-extent aerial view of the Frank Slide. The dashed line below South Peak outlines the area identified by Allan (1931, Figure 2) as being most unstable. Photo reproduced with permission from Alberta Sustainable Resource Development, Air Photo Distribution. Image owned by the Government of Alberta and protected under the Copyright Act of Canada.

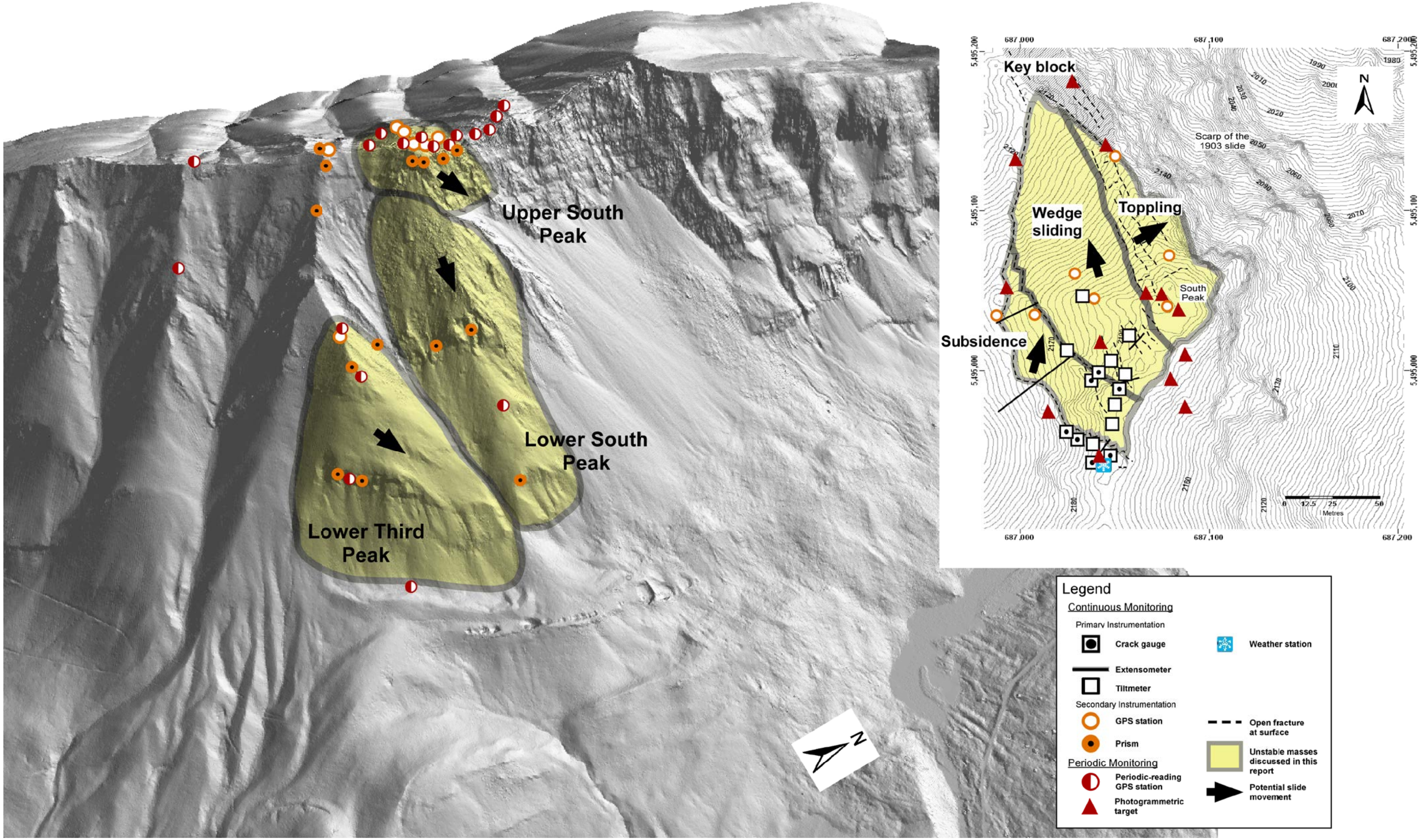

Figure 2. Overview, as of December 2010, of the monitoring network on Turtle Mountain as a whole and South Peak of Turtle Mountain in particular (inset), southwestern Alberta. For better clarity, primary monitoring instrumentation is shown only on the inset.

Figure 3. Physical layout of equipment installed at the borehole datalogging site on Turtle Mountain, southwestern Alberta. Cellular modem can be seen in the lower left (white circle).

2.1.2 Weather Station Upgrade

In addition to recording and telemetering data from the primary sensors, the weather station also provides a platform for collecting basic meteorological data. Sensors used to measure weather data include the following:

- pyranometer (solar radiation)
- barometer (barometric pressure)

- wind monitor
- tipping-bucket rain gauge
- temperature/relative humidity probe
- rock temperature probe

These elements were more than five years old and, upon inspection, some were already showing signs of wear and tear. As a result, it was decided to replace all weather station sensors. New sensors were calibrated and installed during the summer repair campaign of 2010.

The enclosure at the weather station also needed attention. Due to its small size, the equipment and cables inside were arranged in two layers, making any work on this site very difficult. This had been a problem for some time, so a decision was made to replace the old enclosure with a larger one in which all the equipment could be accommodated in a single layer (Figure 4).

The datalogging equipment was also upgraded. The old equipment was obsolete, necessitating replacement with a new model, the CR1000 datalogger. The default setting for this datalogger was for weather sensors to take readings every 5 seconds and for primary sensors to take them every 15 seconds. This was far too frequent, so a new program was written to change the data-collection frequency for all sensors to hourly readings. This will extend the life of the datalogging equipment and reduce the energy consumption of the station, thus reducing demand on the battery.

Figure 4. Physical layout of equipment installed at weather station datalogging site on Turtle Mountain, southwestern Alberta. Limited space in the old enclosure (left) made repair work difficult. The new enclosure (right) is a significant improvement because all equipment is now in a single layer.

2.1.3 Continuous-Reading dGPS Power Supply Upgrade

The majority of the GPS stations on the mountain had been using two 90 A•h 8G27 gel-cell batteries as the storage medium for solar energy. These batteries had reached the end of their useful life and were starting to exhibit power problems. To resolve these issues, the old gel-cell batteries were replaced with new 90 A•h absorbed glass mat (AGM) batteries. These new batteries have several advantages over the gel-cell batteries, including longer expected life (4–6 years) and the expectation that they will perform much better in the harsh environment on Turtle Mountain. To expedite the process of moving almost 950 kg of batteries around the mountain, a helicopter was used to carry them from the South Peak to each of the GPS stations (Figure 5). This methodology worked out quite well: it was both faster and safer than manually moving batteries around the mountain.

During parts of the winter, the amount of solar radiation striking the power-supply-system solar panels can be small. As a result, the dGPS stations were running at the minimum power threshold required to keep the equipment operating for most of the winter. To improve this situation, the pulse-width-modulated (PWM)–type solar controllers were replaced with more advanced, maximum-power-point-tracking (MPPT) solar controllers. The MPPT controllers are capable of delivering significantly more charging current to the batteries when solar conditions are good, allowing for more stored charge on the rare sunny days of winter. This higher efficiency is expected to give the solar systems the extra power required to get through the winter season.

Figure 5. Battery slinging operations, with the helicopter used for battery hauling visible in the middle distance (image taken from a webcam installed on the South Peak of Turtle Mountain).

2.1.4 Replacement of Damaged Continuous-Reading dGPS Units

Both the Lower Saddle and Ridge dGPS units had been offline for some time. These units were visited and replaced during a trip in April 2010. During this expedition, the Upper Saddle dGPS unit was also found to be damaged and was therefore replaced. The damage to these three units was caused by a lightning event in September 2009.

2.1.5 Repair of Primary Radio Link for Continuous-Reading dGPS

Performance of the type of radio being used during the last two years for the Blairmore-Mountain radio link was poor. These radios would stop working for no apparent reason and would remain offline for several hours, with the number of such incidents increasing during the winter season. During the April 2010 field trip, the radios were therefore replaced with a different brand. The initial impression of these new radios is favourable. They are extremely easy to configure and, when installed, they link up immediately. To date, no communication problems have been detected.

In addition to replacing the radios for the Blairmore-Mountain radio link, the power control and monitoring systems at the Mountain radio site were also replaced. The new system should decrease power consumption, increase charging efficiency and provide more detailed information on the status of the power systems.

2.2 Performance

Continuous slope monitoring is very difficult in the harsh and highly variable climate conditions on Turtle Mountain. However, the effects of these adverse conditions on the normal operation of the monitoring system have been minimized with a series of preventive measures. These include frequent sensor inspection, aging-equipment replacement and system modifications. This section provides detailed information on sensor performance in 2010.

2.2.1 Primary Sensors

The Turtle Mountain monitoring system has been operating for more than six years. This has enabled us to understand not only the challenges of maintaining a reliable and essentially continuously running system, but to identify the factors that affect the normal operation of the monitoring network. For the primary sensor network (crackmeters, tiltmeters, extensometers), we find that factors such as high humidity in tiltmeters and snow loading on crackmeters can severely affect these instruments. To mitigate these effects, desiccant packs have been added inside tiltmeter enclosures, and protective roofs were installed over each crackmeter array. The desiccant packs have helped improve sensor reliability considerably; however, the results are not very positive for the protective roofs. Only in a few cases (sets B and C) has the protective roof been able to effectively protect the sensors against snow loading.

Lightning strikes continue to be the main cause of sensor damage. A number of attempts to protect the monitoring system against electrical surcharges associated with lightning strikes have been unsuccessful. An average of two lightning events capable of causing sensor damage are recorded each year.

2.2.2 Secondary Sensors

The secondary-sensor network consists of the electronic distance-measurement (EDM) system and the continuous-reading dGPS system. Operation of these two systems has yielded mixed results. Although the dGPS system performed relatively well during the reporting period, the EDM system has been affected by several factors, such as rain and snow. These factors have introduced large errors into the data or have made prism reading impossible. Given the nature of the site, prisms for the EDM system are also susceptible to damage from falling rocks. Several stations have been damaged because of frequent small rock falls.

All continuous-reading dGPS stations operate using solar power. These monitoring sites were selected for their geological significance rather than their suitability for generating solar power. As a result, some stations receive very little sunlight in winter because the mountain casts a shadow over these areas. This has resulted in momentary losses of power and station shutdown. To address these issues, all aging batteries were replaced with new ones and a series of modifications made to the power-generation and data-recording systems of the dGPS stations. All stations now have a better generating capacity that should keep them operating through the winter.

3 Data Analysis

This section provides interpretations of slope conditions and displacement behaviour based on instrument results, with a focus on only those sensors that operated normally during the reporting period.

3.1 Deformation Monitoring Data

3.1.1 Crackmeters

The continuous-recording crackmeters determine whether the surface fractures open at constant rates or rapidly in one event. However, as already stated in Section 2.2, these sensors are prone to snow or ice loading, which introduces large errors in the readings. Therefore, discussion of displacements is limited to only those arrays that are known to have operated normally (sets B and C).

These instruments provide time series of crack opening and temperature over a period of six years (Figures 6 and 7). Monitoring results show diurnal and annual cycles that correlate with air-temperature cycles. The annual cycles exhibit an active phase, with displacements occurring in early autumn to late winter, and a relatively inactive phase, with limited to no displacement in spring to late summer. Instruments in set B have recorded displacement rates of up to 0.4 mm/year and crack-width changes, related to daily air-temperature cycles, of approximately 0.02 mm.

The fracture-opening measurements from crackmeter set C (Figure 7) also show the very slow long-term trend seen in set B (Figure 6). Examination of the records shows a mean annual displacement rate of <0.4 mm/year; as is the case with set B, this most likely reflects fracture opening due to seasonal air-temperature changes.

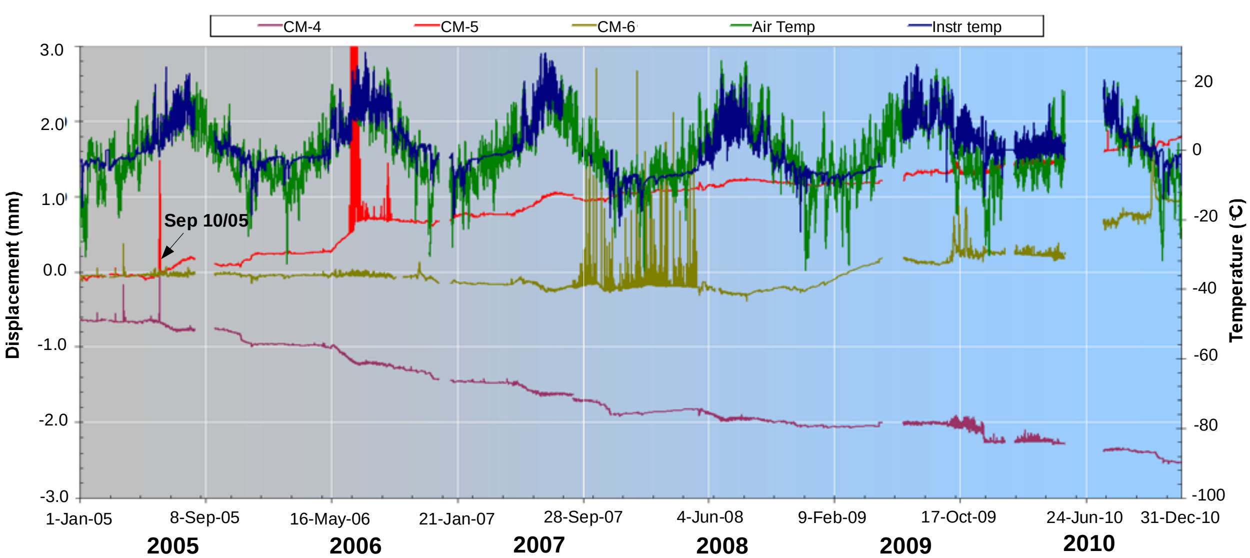

Figure 6. Plot of displacement versus time for crackmeter set B, South Peak, Turtle Mountain.

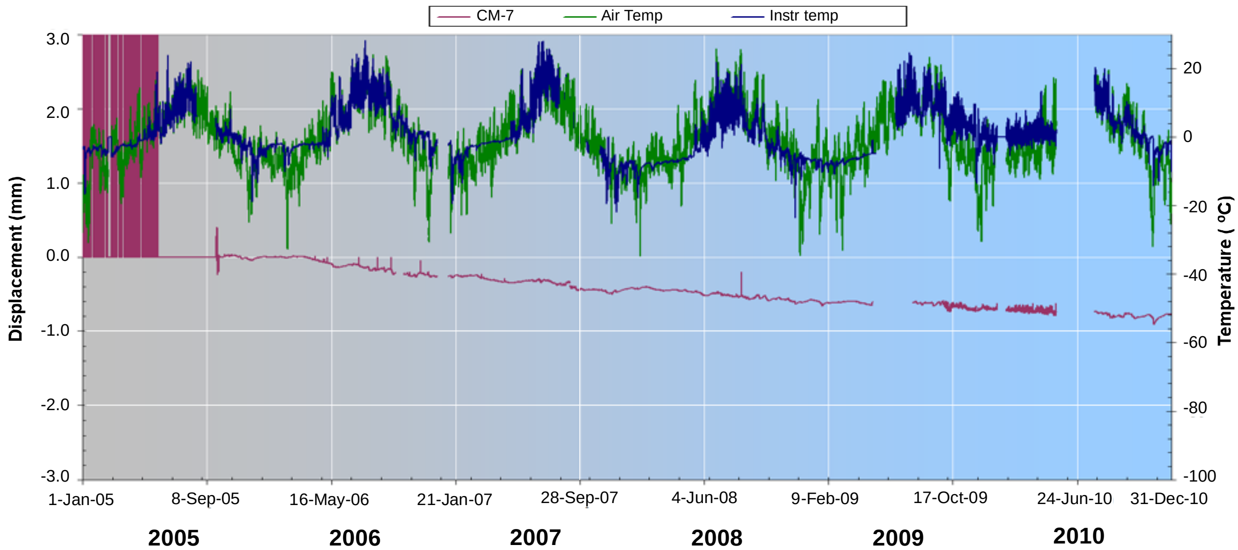

Figure 7. Plot of displacement versus time for crackmeter CM-7 of set C, South Peak, Turtle Mountain.

3.1.2 Tiltmeters

The results from the tiltmeter network are important because they allow an understanding of the rotational component of the displacements. This system, consisting of 10 sensors, was installed during 2005 by AMEC Earth and Environmental (2005). The sensors are in two clusters, one at the sliding wedge and the other at the subsiding zone behind the sliding wedge (Figure 2). Spatial coverage is therefore limited, with no sensors situated within the most active part of the rock mass at the northeastern part of South Peak. The monitoring results between 2005 and 2010 are shown in Figure 8. About half of the sensors show the effects of high humidity inside the instrument enclosure, making the interpretation of small rotations very difficult. In spite of this, some trends can still be identified. In general, all sensors show annual fluctuations, but with no long-term cumulative rotations, and diurnal fluctuations associated with daily air-temperature cycles.

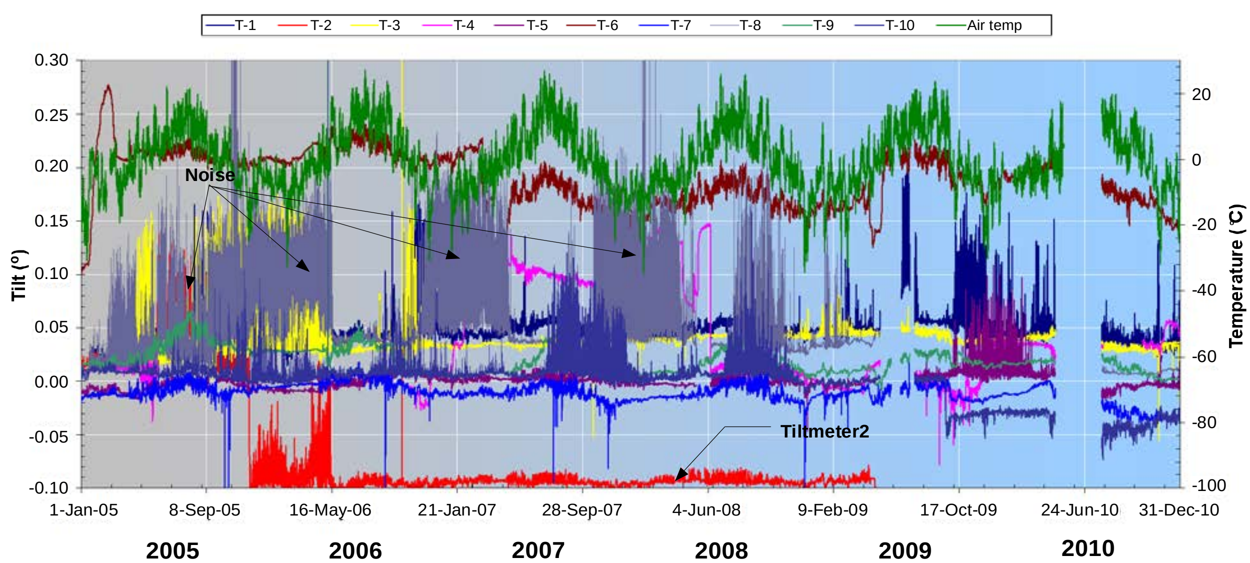

Figure 8. Plot of tilt versus time for tiltmeters, South Peak, Turtle Mountain.

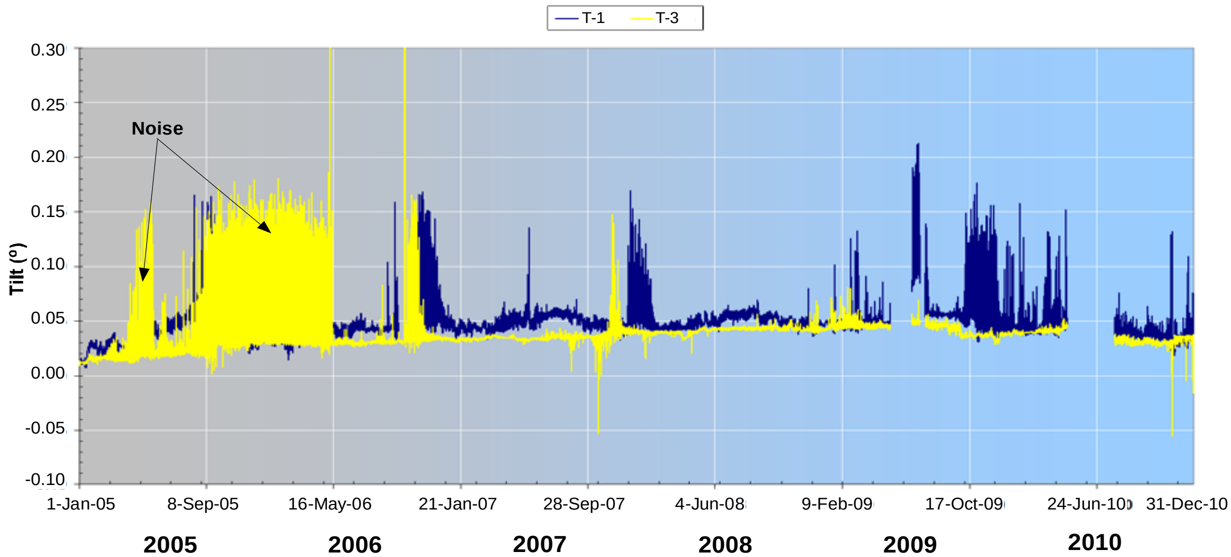

Figure 9. Plot of displacement versus time for tiltmeters T-1 and T-3, South Peak, Turtle Mountain.

Small rotations are found in tiltmeters T-1 and T-3 (Figure 9), with the magnitude and rate of rotation at each station remaining essentially constant for the six-year span of monitoring. This implies that the pattern of deformation of the rock mass has been constant, which is consistent with the trends seen in the crackmeter data.

3.1.3 Extensometers

Displacement versus time plots for all extensometers do not show the cyclical daily and annual fluctuations observed in crackmeter and tiltmeter data (Figure 10). This noticeable difference likely arises from the difference in resolution between the sensor types, with resolution in extensometers two orders of magnitude lower than that of the crackmeters. Extensometers EX-2 and EX-3 continue to be extended at

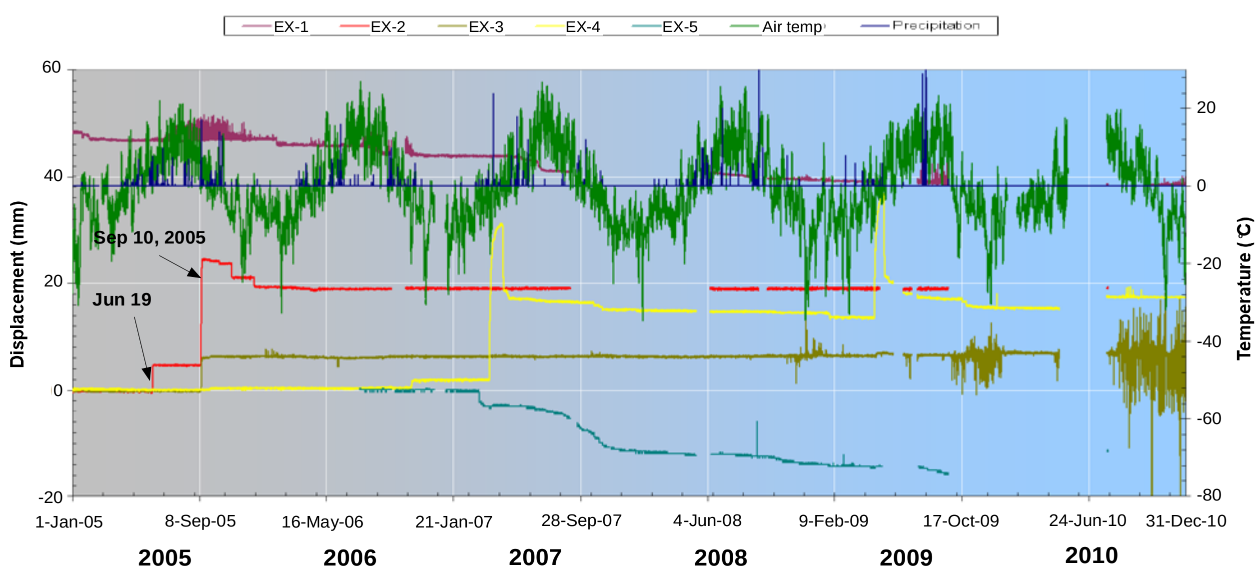

Figure 10. Plot of displacement versus time for extensometers, South Peak, Turtle Mountain.

19 and 6.17 mm, respectively. These displacements were recorded during two periods of heavy precipitation in early June and early September of 2005; Moreno and Froese (2006) discussed the specifics of these events. In addition, the displacement versus time plot in Figure 10 shows a number of transient jumps or steps recorded by sensors EX-4 and EX-5; however, these events are believed to be associated with sensor drift rather than rock displacement. This belief is supported by the fact that no displacement has been recorded by other types of sensors located near EX-4 and EX-5. The exact cause of this sensor drift has yet to be determined, but we believe that it will not affect the sensors' ability to measure real deformations.

3.1.4 Continuous-Reading dGPS Monitoring Network

To determine the detailed history of displacements on active fractures, six single-frequency dGPS stations were installed near prominent fractures (Moreno and Froese, 2008a). These Novatel SuperStar II dGPS units have a resolution in the millimetre range in the horizontal direction and in the centimetre range in the vertical direction. Later in 2008, this network was expanded by an additional four dGPS stations, two on South Peak and two on the middle to lower part of the eastern slope below South Peak (Figure 2). This was done to monitor displacements in areas with the largest movements (South Peak vicinity) or suspected movements (eastern slope) but no previous monitoring (Moreno and Froese, 2009b).

The monitoring results from the dGPS stations are shown in Figure 11. Measurable displacement rates can be seen only at the Lower Saddle and Upper West stations. Annual displacement rates at the Lower Saddle station range mainly between 0.5 and 2 mm/year, which is consistent with previous photogrammetric monitoring (Moreno and Froese, 2006). However, measured displacement orientation appears to be in conflict with the postulated deformation direction for this part of the mountain ('Toppling' area in Figure 2). One must consider that local topography and slope aspects on which the monitoring points are situated will control measured movement directions. As a result, displacement direction measured at some local points might differ from displacement direction for the overall area.

The Upper West station indicates a displacement of more than 6 mm. This is almost certainly incorrect and likely related to a poorly constructed concrete pillar. A detailed onsite inspection of the pillar revealed signs of deterioration; also, the pillar is on heavily broken rock. This material can be very susceptible to freeze-and-thaw events, which can result in large local displacements.

3.1.5 Electronic Distance-Measurement (EDM) System

As discussed in Moreno and Froese (2008b), twenty prisms were installed during the summer of 2007. Figure 12 shows the results of the 15 months of available data. In general, all records show evidence of the annual displacement fluctuation seen most clearly with the crackmeters. However, with the exception of prism PR-15, it is not possible to give a definite magnitude and direction of displacement at this time due to the small scale of the displacements measured.

From May 2008 until October 2008 and from May until November 2009, the system underwent major software upgrades. During this period, data were used only for testing and therefore not written to the main database. As a result we feel we do not currently have sufficient data to resolve any trends.

3.1.6 Ground-Based Interferometric Synthetic Aperture Radar (GB-InSAR)

The peak and eastern face of Turtle Mountain create significant issues for monitoring due to the harsh climatic conditions and the rugged and steep nature of the peak. On an annual basis, snow loading and lightening strikes create ongoing maintenance concerns that require personnel to access the mountain during the summer months and repair sensors in potentially dangerous areas. The use of 'off-mountain' monitoring technologies, such as EDM, is quite limited because of its reliability, since prisms are often

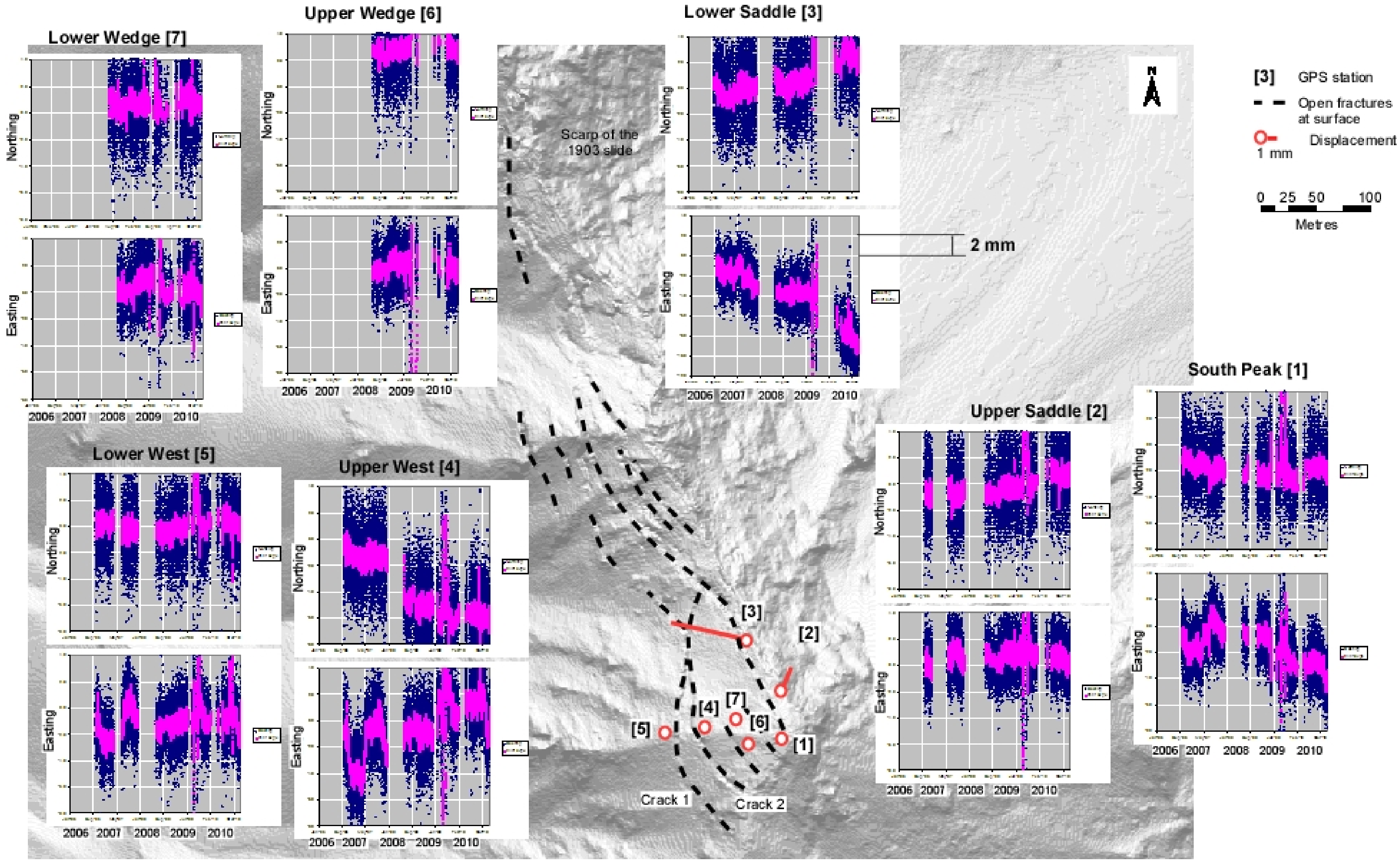

Figure 11. Surface displacements derived from dGPS stations during the period 2006–2008: horizontal component of the surface-displacement vectors (red lines) plotted on a map of the South Peak of Turtle Mountain. The displacement vectors of the dGPS stations are absolute, since they are referenced to an external co-ordinate system. dGPS stations: [1] South Peak; [2] Upper Saddle; [3] Lower Saddle;[4] Upper West; [5] Lower West; [6] Upper Wedge; [7] Lower Wedge.

snow/ice covered in the winter and measurements can only be taken when there is a clear line-of-sight between the prisms and the survey instrument. Therefore, between 2008 and 2010, AGS and its partners began investigating and testing new ways of remotely collecting monitoring data for the east face of Turtle Mountain.

Staff of AGS and University of Alberta researchers came to the conclusion that the most appropriate tool was a ground-based interferometric synthetic aperture radar (GB-InSAR) system. Therefore, such a system (Dehls et al., 2010) has been installed in the valley, approximately 2.7 km east of Turtle Mountain. The principles of this technique are the same as for space-borne InSAR except that, instead of gathering repeat-pass data from satellites orbiting above the Earth, repeat SAR images are collected from 2.5–3.0 km distance from the mountain using a sensor on a rail. This technique originated in Italy and was first reported on in 2004 (Antonello et al., 2004). Initially the technology and available systems had issues with the correction for atmospheric effects and were limited to looking at deformation as a snapshot in time rather than tracking deformation trends. Recent advances in the GB-InSAR processing software and hardware have enabled the collection of more reliable data and tracking of deformations on a pixel-by-pixel basis over time. One of the most significant advantages of GB-InSAR over other laser-type monitoring technologies, such as EDM and terrestrial laser scan (TLS), is that it can obtain data at night and through fog/rain, thus providing a more reliable data stream.

The system at Turtle Mountain was installed at the same location as the total station used for measuring the EDM, a dGPS base station, a meteorological station and a web camera (where visuals of the face of the mountain are collected and archived; Figure 13). The advantage of having the GB-InSAR located with these other monitoring tools, particularly the web camera, is that these other data streams can be reviewed to assess the source of any anomalies in the GB-InSAR data.

At this point, the GB-InSAR monitoring campaign at Turtle Mountain has consisted of a three-month calibration period in the fall of 2009 and a four-month monitoring period in the spring/summer of 2010. In the fall of 2009, the data from the GB-InSAR were compared with the web-camera images and the

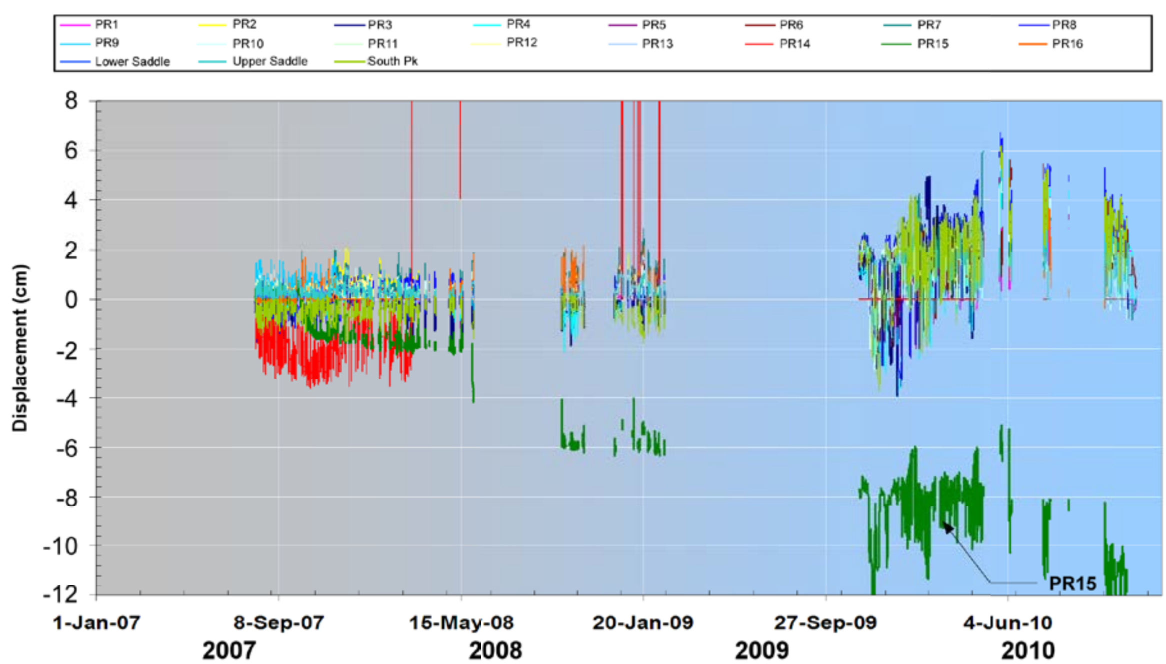

Figure 12. Plot of displacement versus time for electronic-distance-measurement (EDM) prisms at Turtle Mountain.

Figure 13. The IBIS-L GB-InSAR system is installed on a rooftop, facing the unstable slopes on Turtle Mountain. The farthest point on the mountain crest is approximately 3200 m away.

meteorological-station results (from both the base of the valley and the peak of the mountain) to calibrate the system and processing software with respect to the required atmospheric corrections. These corrections were then applied to the readings collected in the spring/summer of 2010, typically the most active time for movements associated with the spring snowmelt.

The readings in the spring of 2010 provided a broader view of the movements on the eastern face, with the main zones of movement observed being on the slowly creeping talus slopes on the lower two-thirds of the face (Figure 14).

3.2 Other Monitoring Data

3.2.1 Climatic and Thermistor Data

Lower maximum (+19.6°C) but higher minimum (–31.8°C) temperatures than in the previous two years (Figure 15) were recorded at the top of the South Peak of Turtle Mountain. Significant daily temperature variations were also common. Rock temperature showed the same general trend as air temperature but was more subdued (lower maximum and higher minimum readings), with a time lag of about 12 hours relative to significant changes in air temperature. Seasonal temperature fluctuations penetrate only about 15 m into the slope (sensor Th-2) and are negligible below that depth, with significant temperature variations measured down to a depth of 8.2 m (sensor Th-4). On the other hand, daily temperature variations are measurable only about 4 m into the slope (Figure 15).

Above-normal precipitation during the reporting period was recorded on the South Peak of Turtle Mountain. Total precipitation in 2010 was 472 mm, 18% greater than the average annual precipitation of 397 mm, which is based on data measured between 1971 and 2000 at the nearby Coleman weather station

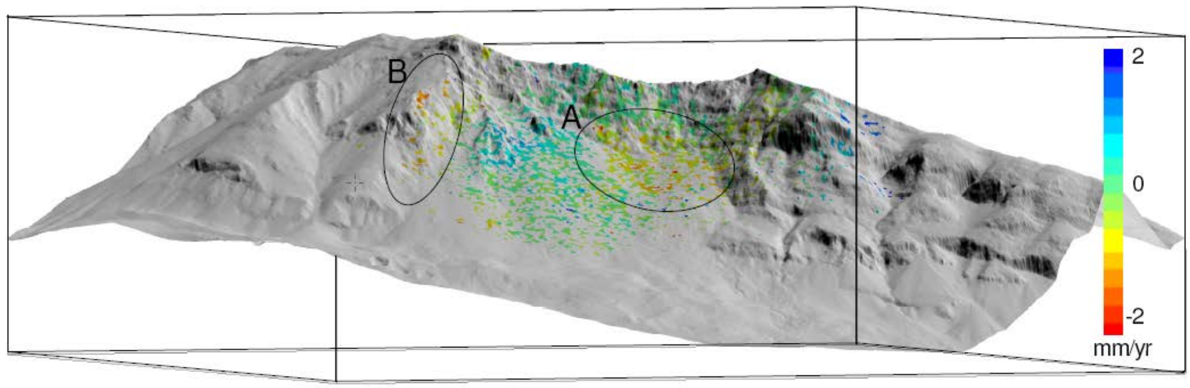

Figure 14. Digital elevation model of Turtle Mountain, as viewed from the instrument location. The colours represent the average velocity along line-of-sight from September 2009 to April 2010. Negative velocities represent movement toward the sensor. Area 'A', in the upper portion of the talus slope, shows increased movement due to oversteepening and continued accumulation from above. Movement in area 'B', on the lower portion of South Peak, is consistent with field mapping in this heavily fractured area.

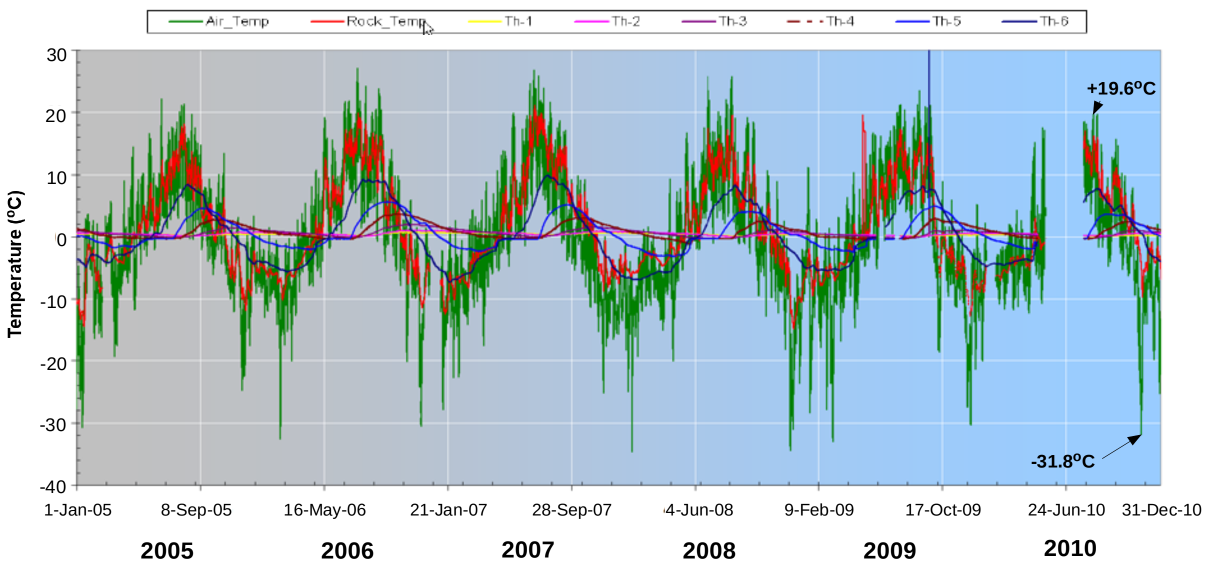

Figure 15. Air temperature and variation of rock temperature with depth in the borehole at the top of South Peak, Turtle Mountain, 2005–2009.

of Environment Canada. Winter precipitation was below normal (Figure 16). Below-normal precipitation was recorded during early spring, whereas an above-normal amount was seen during late spring, which brought the overall precipitation during this season to above normal. Precipitation was above normal for much of the summer but decreased significantly after July 1. Above-normal precipitation was recorded during the fall months (September, October and November).

3.3 Discussion and Interpretation of Monitoring Data

Integration of monitoring and geological data is crucial for assessing the location and extent of the failure surface, and the volume and kinematics of the unstable rock mass. This is an iterative process in which, after detailed geological investigations, possible rockslide scenarios are identified and compared against monitoring data. The comparison results are then used to improve the initially proposed instability

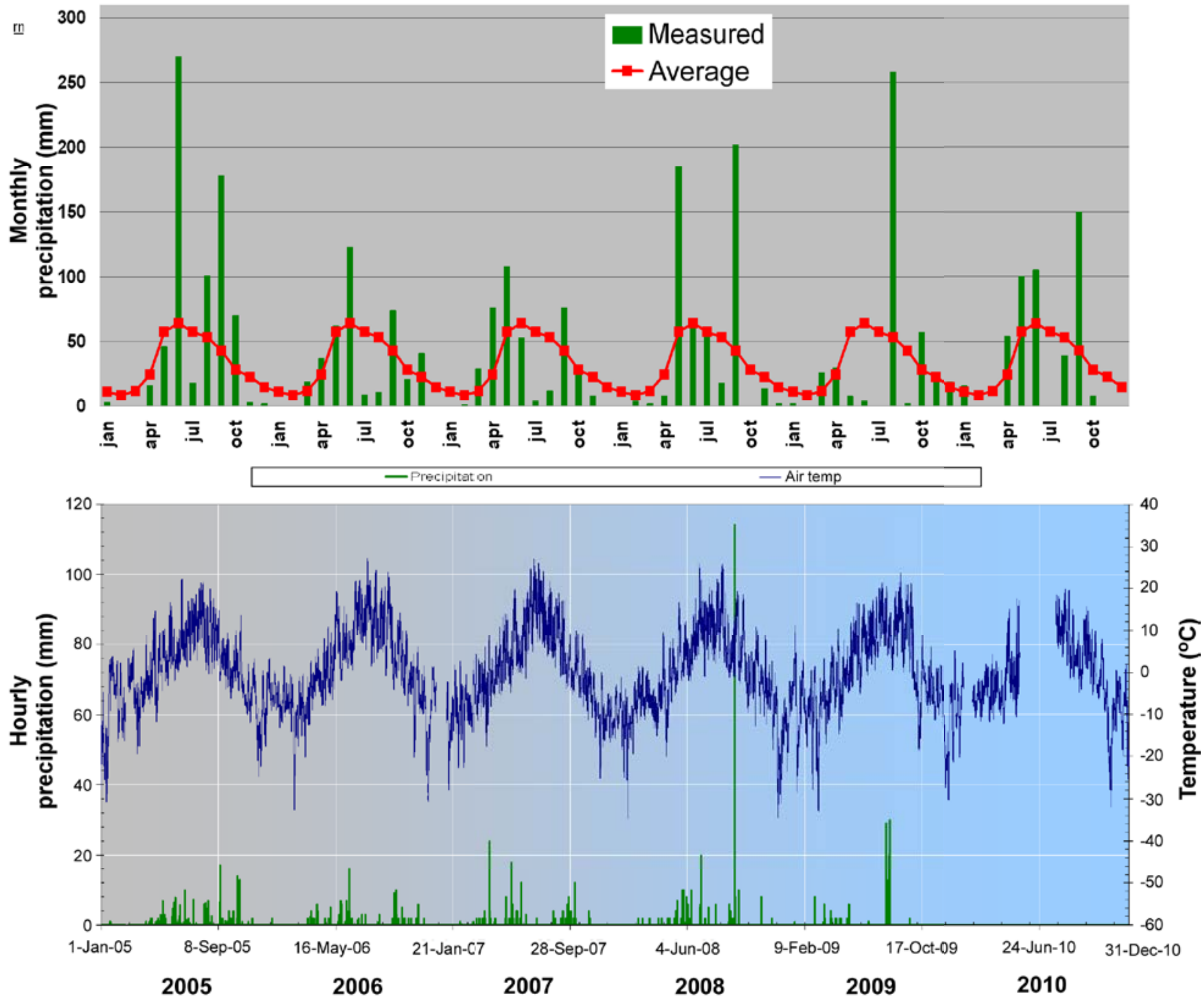

Figure 16. Top: Measured monthly precipitation (2005–2010) and average monthly precipitation (1971–2000). Bottom: Temperature and hourly precipitation near Turtle Mountain, 2005–2010.

scenarios. This process is repeated until an agreement between field and instrument observations is achieved. These derived models will serve as a basis for assigning a geological probability to the possible instability scenarios and to better assess the hazard related to a catastrophic failure.

At Turtle Mountain, monitoring data comprise displacement fields at surface, measured continuously and periodically. Continuous-monitoring data include all data recorded by the primary (crackmeters, extensometers and tiltmeters) and secondary (dGPS and EDM systems) monitoring networks. Data from this group are automatically recorded every hour. Periodic monitoring data consist of displacement measurements of steel target points (periodic-reading dGPS monitoring network) and photogrammetric targets. The steel target network, consisting of 18 points, is surveyed biannually with the help of a high-precision GPS receiver. On the other hand, the photogrammetric-target network consists of 21 targets but only four surveys are available: the initial survey in 1983 and three repeat surveys in 1983, 1984 and 2005. A detailed description of target installation and the methods applied to derive displacement vectors from the displacement measurements of the steel target points and photogrammetric targets is available in Teskey and Ebeling (2010) and Fraser (1983).

Monitoring data are complemented with historical displacement data from monitoring points installed during the brief 1980s monitoring-program effort. These consist of two main components: data from manually read monitoring points (Moiré crack gauges and trilateral signs) and data from remotely measured monitoring points (EDM prisms). These EDM prisms should not be confused with the EDM prism network installed during the period 2005–2007. The prism network installed in the 1980s consisted of three closely spaced targets approximately 10 m below and on the west side of South Peak. On the other hand, the new prism network comprises 20 targets on the eastern face of the mountain and is part of the new monitoring program at Turtle Mountain. For simplicity, targets from the old 1980s monitoring program will be referred to, for the remainder of this report, as the 'old' prisms. Particulars of the 1980s monitoring program and its main components, as well as the monitoring principles, installation details and functionality of these components, are available in Froese et al. (2009).

The questions pertaining to possible rockslide scenarios and their geological controls have been the subject of extensive investigation (Moreno and Froese, 2008b; Pedrazzini et al., 2011). This included fracture mapping across the entire slope in the summers of 2007 and 2008, combined with high-resolution digital-elevation-model (DEM) analyses. According to these studies, there are three unstable blocks that could be involved in a deep-seated multi-block failure. Two are in the area encompassing the South Peak, referred to as the Upper and Lower South Peak instabilities, and a third is in the lower slope below Third Peak (Figure 2).

The following sections focus on the evaluation, using monitoring data, of the different rockslide scenarios for the three identified unstable areas on Turtle Mountain. In the evaluation, the question of how deformation patterns relate to the different slide geometries is addressed by comparing measured displacement patterns with the results of geological investigations. Using this comparison, the number of possible instability scenarios is constrained and reduced.

3.3.1 Upper South Peak

The Upper South Peak represents the main unstable area and has been the focus of the recent monitoring at Turtle Mountain (Moreno and Froese, 2006). Recent field mapping and DEM analyses show that this area is controlled mainly by the discontinuity sets J1, J2, J3 and J6, and the bedding plane (BP). As the orientation of BP and discontinuity J6 are very similar (Figure 17), both are considered to contribute to the basal rupture surface and are treated as one common structural set (BP/J6) in subsequent discussions.

Based on these observations and a movement analysis (Froese et al., 2009), the upper South Peak can be divided into three distinct zones, each one with a particular deformation mode: an eastern toppling zone, a central wedge sliding to the northeast, and a rear subsidence zone. The following sections provide discussion of the displacement patterns obtained in each zone relative to the deformation modes proposed.

3.3.1.1 Zone 1: Toppling

The toppling zone is characterized by linear fractures that trend approximately parallel to the slope face, largely controlled by J2 and locally by J1 and J3. In this zone, the available monitoring points consist of five photogrammetric targets, ten EDM prisms, three continuous-reading dGPS stations and two periodic-reading dGPS station (Figure 2). With the exception of EDM prism PR15, displacement data from the EDM network are on the same order of magnitude as measurement errors and are therefore not included in this discussion. Table 1 provides an overview of the displacements observed for the photogrammetric targets, and Tables 2 and 3 present displacement data for the continuous- and periodic-reading dGPS stations, respectively.

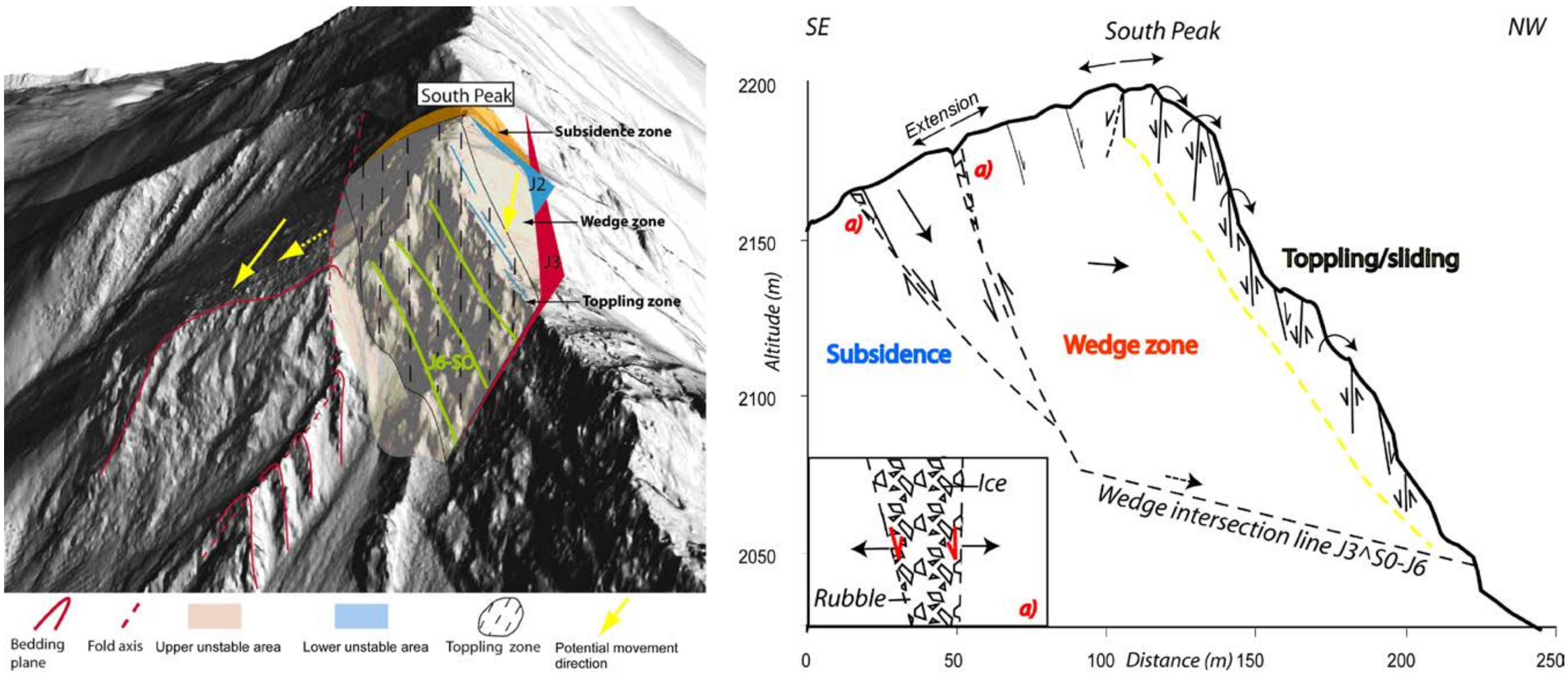

Figure 17. Conceptual model of the unstable area on Upper South Peak, based on structural and monitoring data (Froese et al., 2009).

Table 1. Photogrammetric target displacements between 1982 and 2005, Turtle Mountain.

Zone	Target	Horizontal (mm)	Vertical (mm)	Magnitude (mm)	Rate (mm/year)
1	6	47	74	88	3.8
1	4	30	24	38	1.7
1	18	25	20	32	1.4
1	19	32	20	38	1.7
1	24	19	37	42	1.8
2	20	17	1	17	0.8
3	10	7	8	11	0.4
3	13	15	11	19	0.8
3	21	21	8	23	1.0
Key block	6	47	74	88	3.8
Key block	8	79	18	81	3.5
Key block	9	27	20	34	1.5

magnitude = $((\text{horizontal})^2+(\text{vertical})^2)^{1/2}$
rate = magnitude/number of years

Table 2. Continuous-reading dGPS station displacements between 2005 and 2010, Turtle Mountain.

Zone	Station	Horizontal (mm)	Vertical (mm)	Magnitude (mm)	Rate (mm/year)
1	Lower Saddle	8.2	9.0	12.2	2.3
1	Upper Saddle	2.2	6.0	6.4	1.2

Table 3. Periodic-reading dGPS station displacements between 2008 and 2010, Turtle Mountain.

Zone	Station	Horizontal (mm)	Vertical (mm)	Magnitude (mm)	Rate (mm/year)
1	Point 1	8.2	11.0	13.7	2.0
1	Point 2	6.4	- (1)	6.4	3.2
2	Point 15	8.7	- (1)	8.7	4.4
Key block	Point 12	4.6	- (1)	4.6	2.3
Key block	Point 13	- (1)	- (1)	- (1)	- (1)
Key block	Point 14	- (1)	- (1)	- (1)	- (1)
Key block	Point 17	5.0	- (1)	5.0	2.5

(1) no measurable displacement

In general, there is a good agreement between the results from periodically read monitoring points and those obtained from the continuously read sensors. Both sets of monitoring data indicate that a combination of toppling and planar sliding of these blocks is occurring, which confirms field observations and kinematic analysis completed in this area. Average displacement rates for this zone range between 1.2 and 3.8 mm/year.

3.3.1.2 Zone 2: Wedge Sliding

This zone covers the largest unstable area delineated on the South Peak. It is controlled by the BP/J6 discontinuity along the western limb of the Turtle Mountain anticline and either discontinuity J2 or J3, as shown in Figure 18. Differentiation between a J2^BP/J6– and a J3^BP/J6–controlled wedge will be dependent on the location of the moving portion of Zone 2 relative to the surface topography. Location of the J2^BP/J6 (Zone 2A) and J3^BP/J6 (Zone 2B) wedge sliding zones is provided in Figure 18.

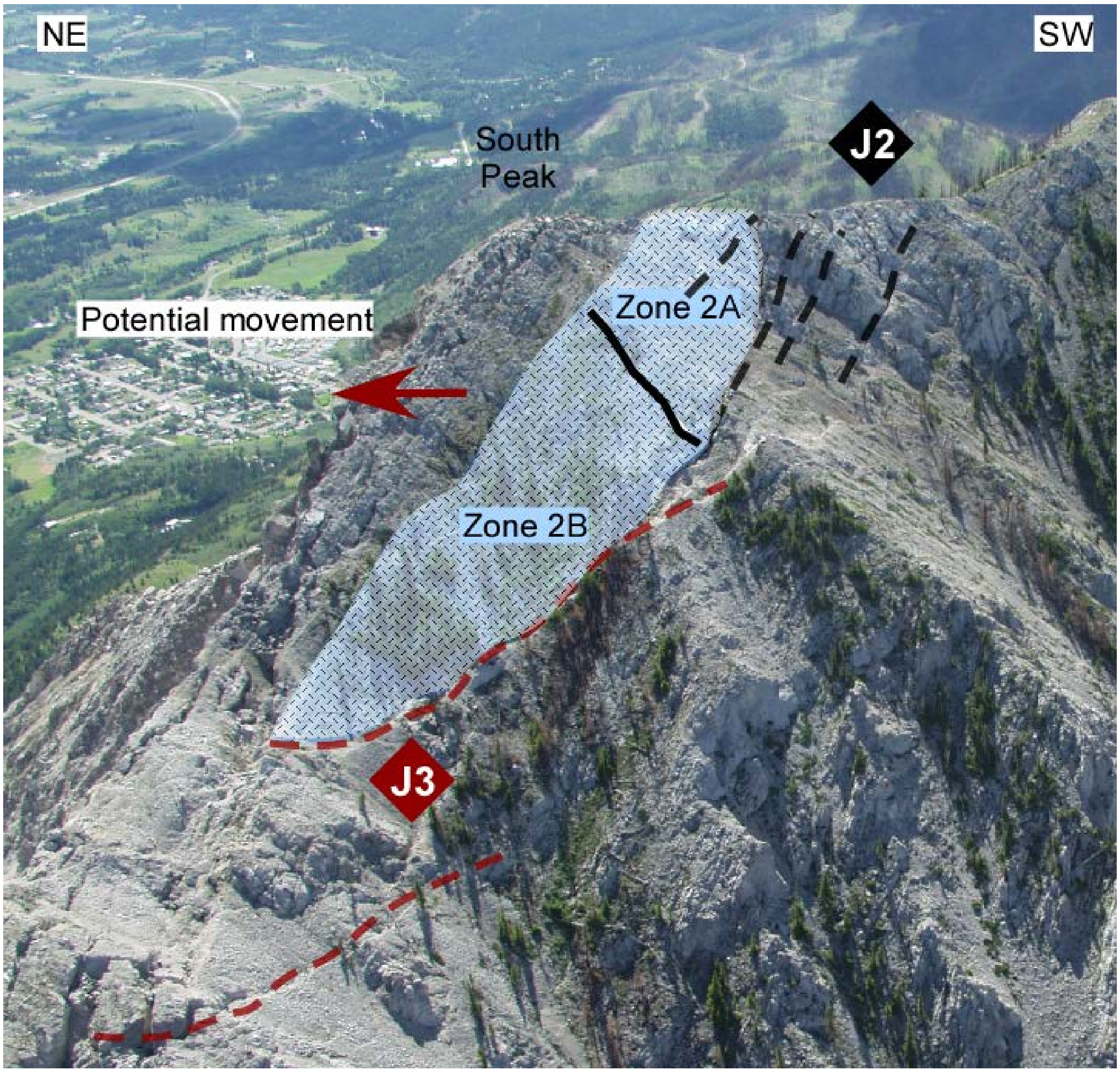

Figure 18. Close-up of the postulated wedge-failure zone. This zone is bounded by joint sets J2 and J3, and, at the base, by the bedding plane on the western limb of the Turtle Mountain anticline.

Monitoring in this zone initially consisted of four tiltmeters, two extensometers and one crackmeter set, most of them in Zone 2A. This network was extended to Zone 2B in 2007 with the addition of two periodic-reading dGPS stations and, in 2008, with the addition of two continuous-reading dGPS stations. Monitoring is complemented with one photogrammetric target (P-20). Unfortunately, most of the sensors display different degrees of noise in their readings, which makes small displacements almost impossible to detect. Therefore, discussion of displacements is limited to only those sensors that are known to have operated normally (T-1, T-3, set B, Point 15 and P-20).

Monitoring results show that displacement rates vary from 0.2 to 0.8 mm/year (Tables 1–4) and that the deformation mode is predominantly translational, most likely on a bedding-controlled rupture surface. This is consistent with the deformation mode highlighted by kinematic analyses and field mapping. Magnitude of rotation derived from tiltmeters T-1 and T-3 indicates that deformations on the mountain are essentially constant over time (Figure 9), which is in accord with the displacement style observed on other sensors. Unfortunately, the tiltmeters used on the mountain are one-dimensional (1-D) sensors, and therefore cannot provide complete information about the three-dimensional (3-D) nature of displacements (deformation mode).

Table 4. Crackmeter displacements between 2005 and 2010, Turtle Mountain.

Zone	Set	Horizontal (mm)	Vertical (mm)	Magnitude (mm)	Rate (mm/year)
2	B (1)	2.1	1.7	2.7	0.5
2	C (2)	-	-	1.0	0.2

(1) array of three crackmeters (CM-4, CM-5 and CM-6) installed at this location to determine 3-D displacement vector
(2) only one working sensor (CM-7) available

3.3.1.3 Zone 3: Subsidence

This zone corresponds to an area of heavily fractured rock that appears to have subsided, mainly on the discontinuity set J2, as a result of lateral displacement of the wedge zone. The total volume of the subsidence zone is estimated to be 0.25–0.45 million m^3.

Sensor installation of the 1980s monitoring network was based on the assumption that the large fissures on the top and west side of South Peak were the head of a large (approximately 5 million m^3) mass that was moving to the east. Initial installation of the new monitoring network was also based on the same assumption. As a result, many of the monitoring points were placed in this zone (Figure 19). Monitoring in this zone includes all of the historical monitoring points and most of the new monitoring-network sensors. Table 5 presents a detailed list of all monitoring points in this area.

Table 1 provides an overview of the displacements observed on the photogrammetric targets, and Table 6 presents displacement data for the Moiré crack gauges.

There is good agreement of the results from photogrammetric targets P13 and P21 with those obtained from the two Moiré crack gauges. Both sets of instruments indicate deformations that are both down and into the slope (to the south-southeast) and are consistent with visual observations that this highly broken zone is subsiding into the void created by the sliding wedge that forms Zone 2. In addition, the results from the readings of the EDM prisms between 1982 and 2006 indicate a decrease in crack width between targets A and C, rather than the opening that was expected when these targets were originally installed. In

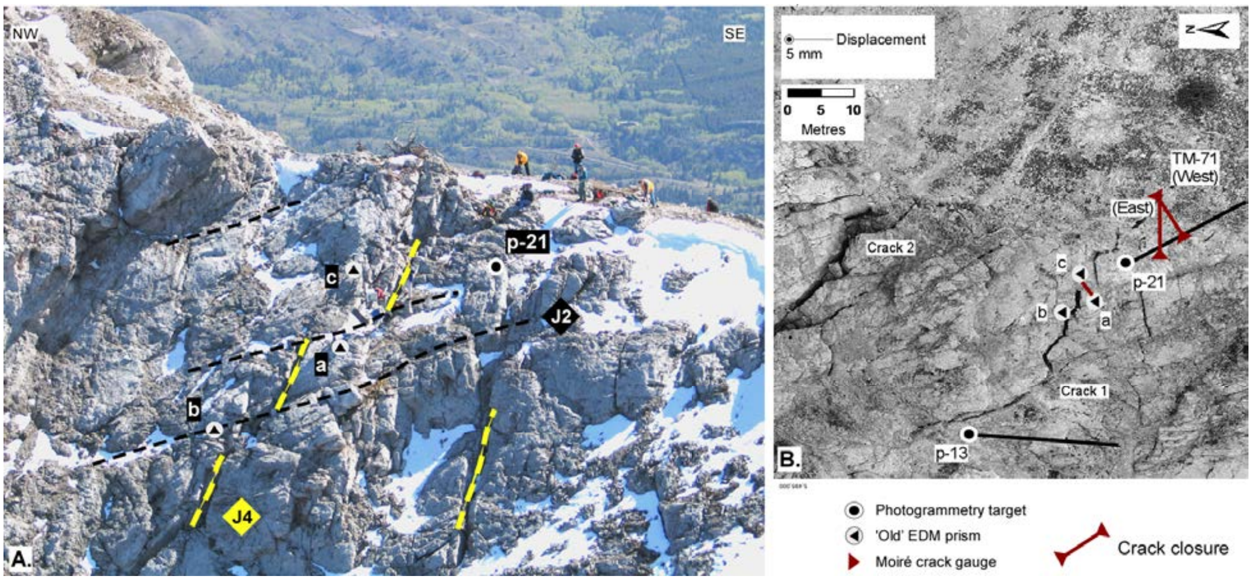

Figure 19. A) Close-up of the postulated wedge-failure zone. This zone is bounded by joint sets J2 and J3, and, at the base, by the bedding plane on the western limb of the Turtle Mountain anticline (Froese et al., 2009). B) Horizontal displacement vectors of measured displacement in the subsidence zone.

Table 5. Monitoring points in the subsidence zone.

Historical monitoring points:

Sensor type	Quantity
Moiré crack gauge	2
'old' EDM prism	3
Trilateral sign	14

New monitoring points:

Sensor type	Quantity
Photogrammetry target	2
Tiltmeter	6
Extensometer	3
Crackmeter	17

Table 6. TM-71 gauge displacements between 1981 and 1994 for the Zone 3 area, Turtle Mountain.

Gauge	Horizontal (mm)	Vertical (mm)	Magnitude (mm)	Rate (mm/year)
Eastern	3.17	0.94	3.2	0.24
Western	4.58	0.96	4.6	0.33

contrast, tiltmeters, crackmeters and extensometers offer little quantification of the magnitude and direction of movement. Although crackmeters are prone to snow or ice loading, which introduces large errors in their readings, tiltmeters and extensometers can only offer an accurate history of displacement in one direction. Unfortunately, all of them are incorrectly oriented relative to the main direction of movement, as they were installed based on the assumption of an easterly moving South Peak.

3.3.1.4 Saddle – Key Block

Although not a part of the South Peak instability volume, this block plays a key role in the wedge-failure mechanism for Zone 2. Looking at the wedge zone, it is apparent that the toe of this feature is at least partially buttressed by the highly fractured material at the head of the 1903 slide. This zone is commonly referred to as the saddle between North Peak and South Peak (Froese et al., 2009). Kinematic analyses reveal that a toppling failure mechanism controlled by J2 and J3 sets is possible, along with wedge sliding on J1^J3 intersection lines.

Three photogrammetric targets and three periodic-reading dGPS stations are in this zone. Recorded displacements of these targets and dGPS stations are presented in Tables 1 and 3, respectively.

As shown in these tables, deformations in Zone 4 have higher velocities than those observed in the other three zones. Deformations of 81–88 mm (3.5–3.8 mm/year) were observed on the photogrammetric targets between 1982 and 2005. Target P8, approximately 60 m from the eastern face, is moving predominantly by translation and P6, within 12 m of the exposed eastern face, has a significant downward component to its movement. Similarly, the results from the periodic dGPS stations show that only the two points in the base of the saddle (points 13 and 14) have not moved relative to each other. All other points on the north and south sides of the base of the saddle (point 17 on the north side, and points 1, 15, 2 and 12) have moved into the saddle. In this zone, large blocks fall annually, leaving fresh debris tracks on the upper portion of the Frank Slide debris field (Froese et al., 2009).

3.3.2 Lower South Peak

The lower portion of South Peak is characterized by abundant rock-fall activity and heavy fracturing that trend southeast, generally parallel to the J2 discontinuity set. Based on the fracture-network orientation as inferred from surface mapping and kinematic analyses, at least six different potential rockslide scenarios can be identified in this area (Figure 20). All the zones appear to be moving toward the northeast, mainly following the J1 discontinuity set. The rear limit of the blocks is defined by the J2 discontinuity, whereas the BP plays the role of lateral limit. Large-scale movements in the slope direction following the wedge J2^J3 are kinematically possible, but field mapping provided no evidence of such type of movement. Potential unstable volumes are estimated to be 0.12–5.5 million m^3.

In this zone, the available monitoring points consist of only three EDM prisms and two periodic-reading dGPS stations (Figure 2). Unfortunately, as measurement errors are on the same order of magnitude, the results from the EDM prisms and dGPS target points cannot be used to determine movements on the mountain. More data over a longer period will be required to resolve any trends.

3.3.3 Lower Third Peak

Geological investigations in the lower Third Peak area resulted from the discovery of two significant fractures in its upper part (Figure 21). These fractures show movement to the northeast, with accumulated displacements of approximately 20 cm (Pedrazzini et al., 2011), suggesting a reactivation of discontinuity set J2. Kinematic analyses and measured displacement vectors of the cracks reveal that different potential rockslide scenarios are possible, one a deep-seated gravitational slope (DSGS) deformation and several superficial unstable masses (Figure 21). The large instability can be well differentiated in its upper part, but the lateral and toe limits are difficult to define, either in the field or by

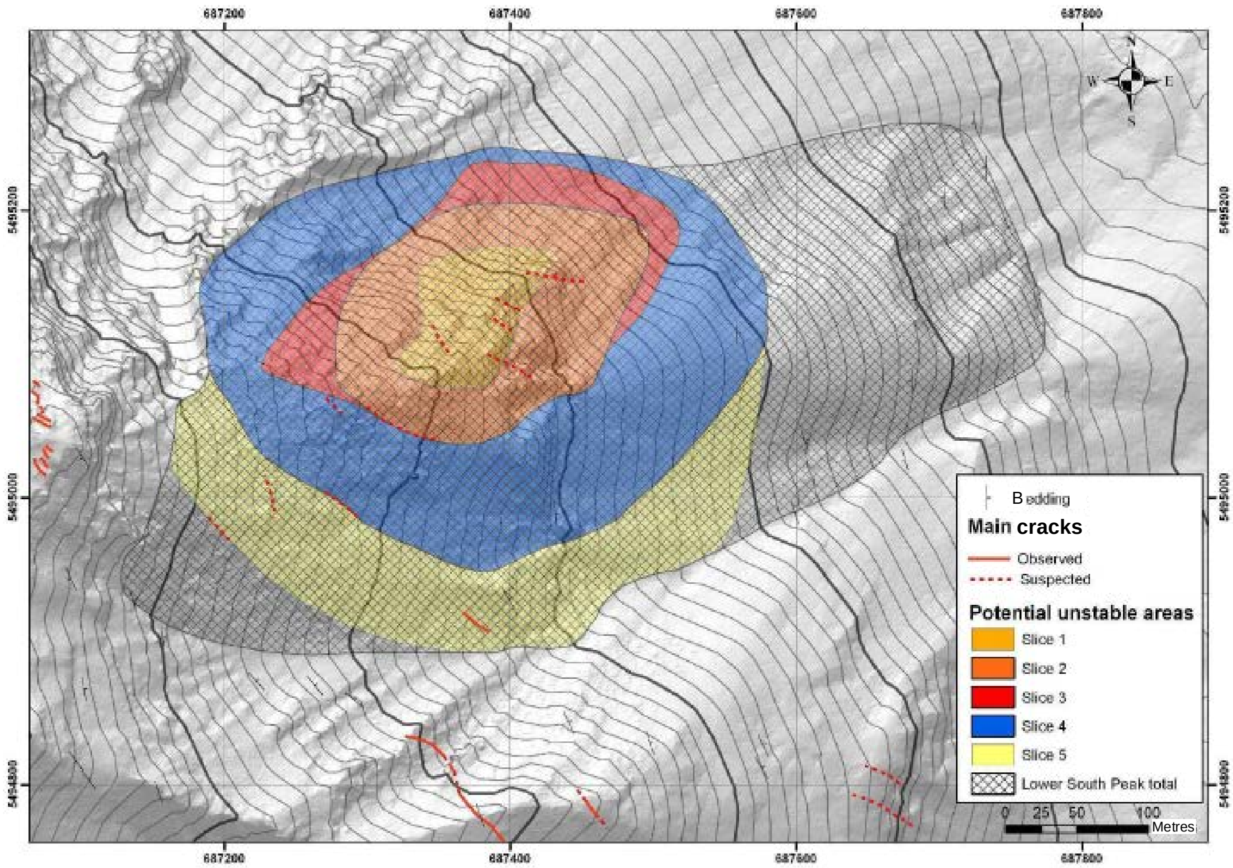

Figure 20. Instability areas detected in the lower South Peak area (Pedrazzini and Jaboyedoff, 2008).

DEM analyses. The most likely mechanism for these two unstable blocks corresponds to a planar failure following the J1 discontinuity, with the BP acting as a lateral release surface and J2 playing the role of rear limit. Other kinematically possible sliding mechanisms include wedge failure formed by the J1^J3 or J2^J3 discontinuities; however, this type of mechanism could not be recognized during field mapping. Calculated volume for the DSGS area ranges between 1.9 and 2.2 million m^3 (Pedrazzini and Jaboyedoff, 2008). However, this estimate can be taken only as rough approximation of the potential unstable volume due to the difficulty in identifying the limits of the instability. The volume of the small superficial unstable area was estimated to range between 0.57 and 0.85 million m^3 (Pedrazzini and Jaboyedoff, 2008).

In this zone, the available monitoring points consist of four EDM prisms and one continuous-reading and four periodic-reading dGPS stations (Figure 2). These points were added after field mapping and kinematical analyses highlighted the potential for a large rock avalanche and recommended the expansion of the monitoring system to this area. Displacement observations began in the summer of 2007 for the EDM prisms and periodic-reading DGPS stations, and in the summer of 2008 for the continuous-reading dGPS station. Unfortunately, no conclusions regarding the style and rate of displacement in this area can be drawn from the existing monitoring points. Analysis of the monitoring data reveals that displacement measurements are not significant relative to calculated measurement errors. As a result, they cannot be used to determine movements on the mountain. More data over a longer period will be required to resolve any trends.

4 Supporting Studies and Research

4.1 Field Analysis of Frank Slide Debris

Rock avalanches are very complex slides that are not yet fully understood. As these events are rarely witnessed, most of the studies on avalanches have been conducted on past events. However, the great majority of avalanche studies has focused on the triggering factors. As a result, the factors that influence the propagation of a rock avalanche have not been completely recognized. Presently, none of the proposed explanations for the high mobility of rock avalanches are accepted by the scientific community and are therefore actively debated (Heim, 1932; Kent, 1966; Hsu, 1975; Goguel, 1978; Melosh, 1987; Dade and Huppert, 1998). Thus, a better understanding of the rock-motion phenomenon is crucial for the development of a model that reliably predicts avalanche runout. One approach to advance our knowledge is to make a detailed description of the morphological and depositional features of rock avalanches. However, analysis of real deposits is generally carried out on photographs rather than by field observations because the latter can be difficult to conduct due to access and time constraints.

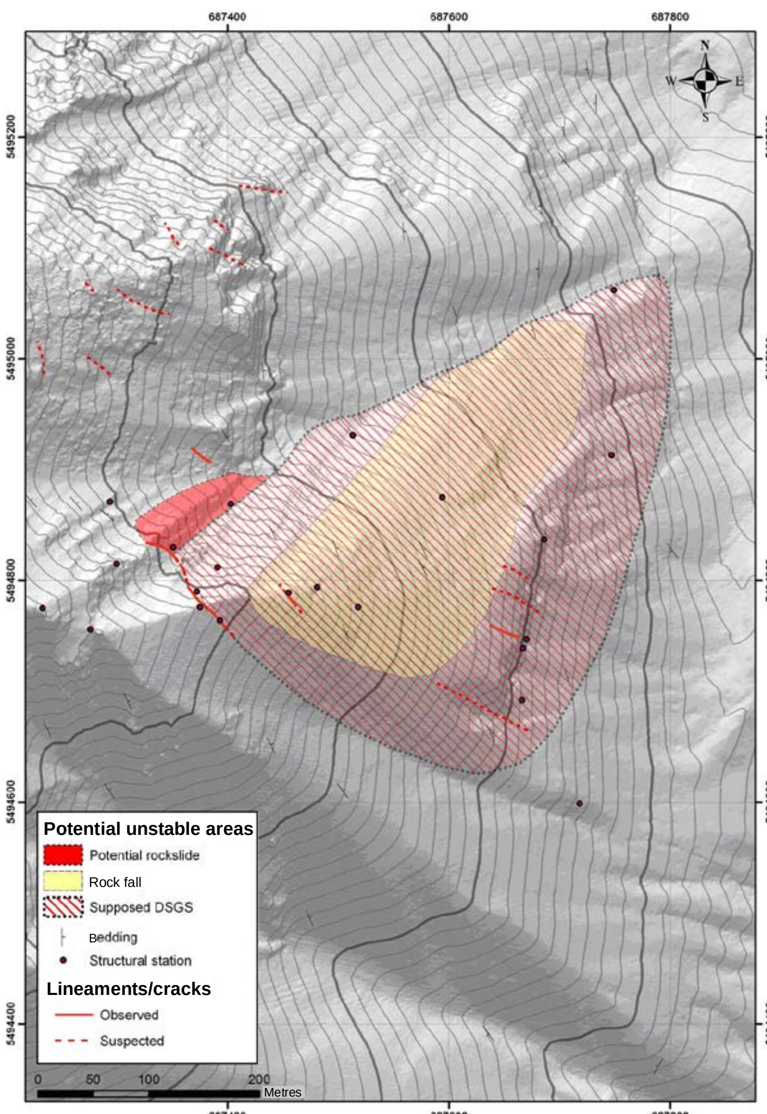

Figure 21. Instability areas detected in the lower Third Peak area (Pedrazzini and Jaboyedoff, 2008).

The Frank Slide debris field presents a unique opportunity to conduct a field survey due to its ease of access. Therefore the University of Lausanne (Charriere, 2011) carried out a detailed description of the slide deposit based on field observations. Fieldwork consisted of describing the deposit's surface in terms of the variables

- mean diameter,
- lithology, and
- orientation of the major axis.

Work was completed during the summer of 2010 and the results will be reported in the 2011 yearly summary report.

4.2 Periodic-Reading dGPS Monitoring Network

In May 2007, the University of Calgary Geomatics Engineering Department, in collaboration with AGS, started the monitoring of two areas on the mountain that were highlighted by recent field mapping as potentially unstable zones (Moreno and Froese, 2008b). The first area is within the active parts of the Saddle zone, between South and North peaks; the second is the eastern face of the mountain (below Third and South peaks). The monitoring network initially consisted of 14 steel targets but was expanded to 18 targets during the summer of 2008 (Figure 2). It is expected that this layout will provide the coverage required to detect and characterize displacement patterns in these potentially unstable areas.

In general, two sets of observations are made every year at all 18 target points, one during early summer and a second in late fall. These observations are taken using two types of device: a high-precision total station (HPTS) and a differential Global Positioning System (dGPS) instrument. Initial dGPS and HPTS readings were taken during June 2007 and then repeated in 2008, 2009 and 2010 (Table 7). To fully correct for sensor effects, measurements at selected points that are considered stable relative to those on South Peak are taken during every observation campaign. These readings are used to calculate correction factors, and these factors are then used to correct the measurements of the other target points.

To determine movements, a multi-parameter–transformation (MPT) mathematical model was applied (Teskey and Ebeling, 2010). This model, which relates initial and subsequent readings connecting base stations and target points, was applied to independently analyze both dGPS and HPTS measurements. The results show that apparent movements calculated at all target points are less than the potential dGPS measurement error, so they cannot be considered statistically significant (i.e., no movement detected). On the other hand, analysis of HPTS measurements confirms the existence of movements in the Saddle area between North Peak and South Peak. These movements are consistent with a slumping and sliding movement, which agrees quite well with independent tilt measurements taken on target points in the Saddle area by Teskey and Ebeling (2010).

Displacement monitoring will continue through 2011 and is expected to go on for years to come. We expect that this continued monitoring will provide us with the data required to refine our understanding of movements on the mountain.

Table 7. Target point readings during the period 2007–2010.

Differential Global Positioning System (dGPS):

Year	No. of Reading Campaigns	No. of Targets Read	No. of Base Stations
2007	2	14	1
2008	2	18 (5) (1)	1
2009	1	18	3
2010	1	18 (2)	3

High-Precision Total Station (HPTS):

Year	No. of Reading Campaigns	No. of Targets Read	No. of Base Stations
2007	2	14	2
2008	2	7 (3)	1
2009	1	7 (3)	1
2010	1	7 (3)	1

(1) subset of dGPS observations made in September 2008 at target points in the saddle between North and South peaks
(2) dGPS observations made for a 24-hour period
(3) HPTS observations made only at target points in the saddle between North and South peaks

5 Summary

5.1 Sensor Network

Analysis of the data from the near–real-time monitoring system and other studies of Turtle Mountain are ongoing. The monitoring system continues to be optimized to focus on sensors and technologies that provide the most reliable and accurate record of movements on the mountain. Recent advances in understanding the movement mechanisms on South Peak and other portions of the mountain by Pedrazzini and Jaboyedoff (2008) and Froese et al. (2009) mean that our understanding of the value of the data from the various instruments is also changing. For example, when we installed sensors during the period 2003–2005 (Moreno and Froese, 2006), we assumed that the large fissures on the top and west side of South Peak were the head of a large (approximately 5 million m^3) mass that was moving to the east. As demonstrated by Froese et al. (2009), the upper part of South Peak is more likely moving as three masses. This means that much of the instrumentation was installed in a rubbly zone of subsidence, making many of the crackmeters and tiltmeters of little use for prediction and warning because they reflect the subsidence and/or are oriented incorrectly to detect and quantify direction of movement.

Based on these findings, the focus shifted to monitoring of a wider area on the eastern face of Turtle Mountain, as described by Moreno and Froese (2008b). This focus shift involved incorporation of dGPS, laser-ranging technologies and GB-InSAR to monitor movements of the various blocks. We consider the dGPS technology most promising as an ongoing monitoring tool because 1) displacements measured by the dGPS system are relative to a geographic reference system rather than to the installation orientation of the device (as is the case with the laser-ranging and GB-InSAR technologies); 2) it can operate under various weather and visibility conditions; and 3) it can provide high-resolution (order of millimetres) displacement data.

5.2 Risk Management

Following the 1903 slide, the initial focus of concern regarding a second large rock slide was on North Peak. In 1912, following a report by Daly et al. (1912), it was deemed that the North Peak of the mountain was unstable, so the remaining portions of the town of Frank were moved. It was not until 1931 that Allan (1931) identified a large unstable volume (up to 5 million m^3) below South Peak and developed the first map outlining the potential zone that would be impacted by a failure of South Peak. Although there are no specifics given on the methods used by Allan, it is suspected that he used the evidence from the runout of the 1903 slide and applied these empirical relations (upper and lower bounds) to the existing topography of South Peak to estimate bounds for runout of debris. In 1999, the Government of Alberta contracted BGC Engineering to reassess the validity of Allan's proposed failure volume and mechanism, and to update the estimates for the spatial extent of the runout based on modern empirical techniques. There was only limited scope for the use of runout modelling during this study.

In 2008, in tandem with the work being undertaken on the estimates of unstable volumes by the University of Lausanne (Pedrazzini et al., in press), new forward dynamic models (both 2-D and 3-D) were applied (Hungr, 2008) and led to an updated understanding of the debris mobility and potential affects on local land-use planning.

Several new areas of potential instability have been discovered on Turtle Mountain, as described in the previous sections and reported in (Figure 22), in addition to the area initially recognized by Allan (1931).To determine the significance of these potential landslides on planning for emergency response

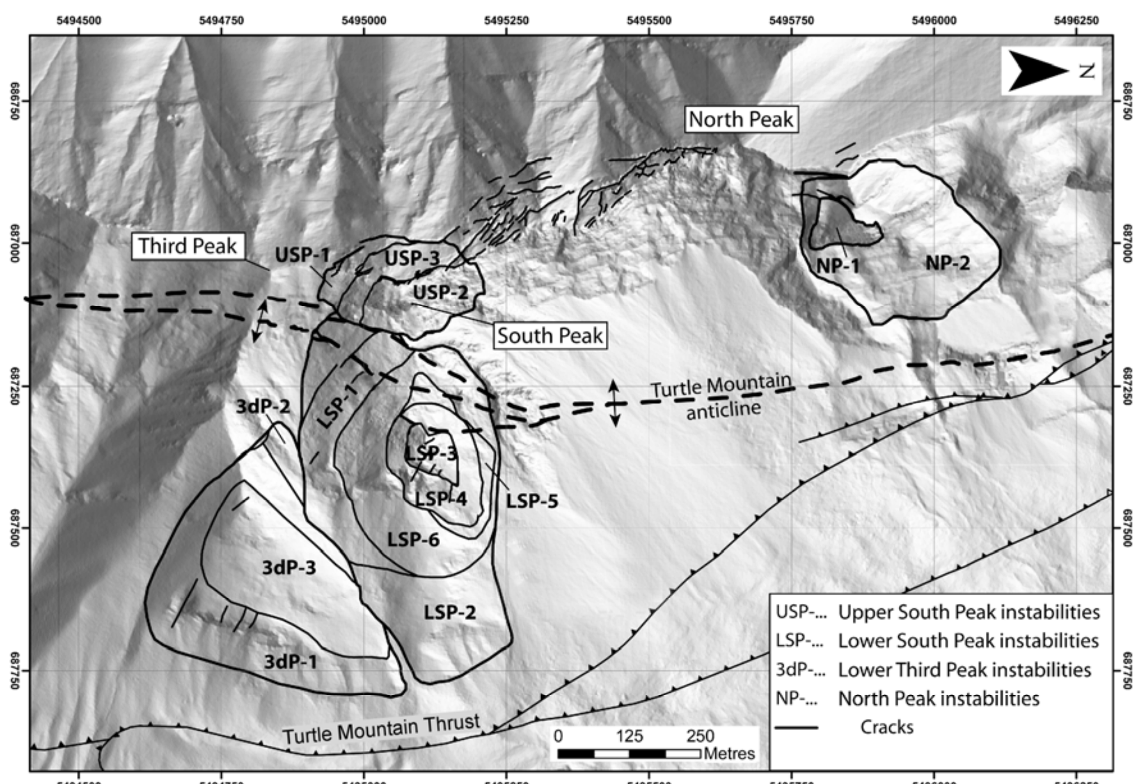

Figure 22. Outlines of the 14 unstable zones identified in the Third Peak, South Peak and North Peak areas of Turtle Mountain (modified from Pedrazzini et al., 2011).

and land use below the eastern slopes of Turtle Mountain, the specific runout scenarios for the various zones needed to be determined. In the time that has passed since previous hazard-characterization studies (Allan, 1931; BGC Engineering, 2000), new numerical methods of landslide motion analysis have been developed and tested. As part of the recent studies, two such numerical models have been used to estimate the possible consequences of the potential failures that have been identified (Hungr, 2008). Analyses were completed using both a three-dimensional (3-D) model, DAN3D, and a two-dimensional (2-D) model, DAN-W. The two models were calibrated by back-analysis of the 36 million m^3 1903 Frank Slide and other smaller rock avalanches. A summary of the maximum runout distances from the 2-D and 3-D analyses of the 12 new source zones is given by the maximum runout envelopes in Figure 23. The 2-D maximum runout distances are typically somewhat longer than the 3-D results due to the concentration of energy in a narrow path. The direction of movement of the 3-D slide and the assumed 2-D profile often did not agree, showing the sensitivity of the 3-D models to topographic details. As shown on Figure 23, the limits to both the 3-D and 2-D analyses for the piecemeal failure of the 12 separate volumes is less extensive than the previous limits outlined by Allan (1931) and BGC Engineering (2000), and therefore present a more optimistic case for considering land-use restrictions in the valley bottom.

6 Conclusions

The large slope instabilities that affect the eastern portion of Turtle Mountain have fascinated more than three generations of scientists. Our understanding of the geology and related slope instabilities has continuously evolved through time. The recent application of modern characterization, monitoring and modelling technologies has greatly increased our understanding of the 1903 Frank Slide and of the

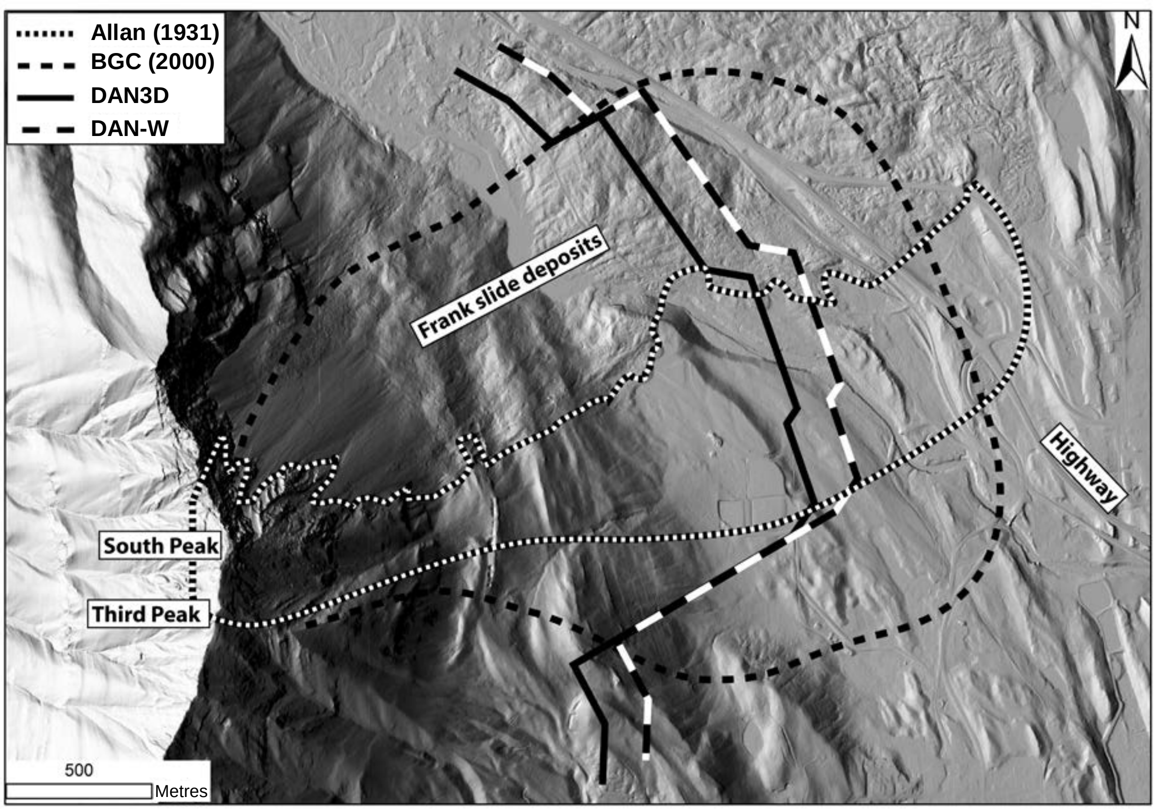

Figure 23. Updated runout scenario envelope compared to the previous estimates for a single large event from South Peak and Third Peak. Adapted from Pedrazzini et al. (in press). Abbreviation: BGC, BGC Engineering Inc.

existing rock-slope hazard at Turtle Mountain. New geospatial modelling tools, coupled with a high-resolution LiDAR digital elevation model (HRDEM) and field mapping, have allowed a detailed structural evaluation of the entire mountain and new interpretations of the potentially unstable zones and their volume.

Detailed structural analysis highlights the influence of folding and post-folding deformations on the development of brittle-rock tectonic features that played a primary role in the development of the 1903 rock avalanche event and continue to do so in the observed displacement directions of current potential instabilities.

The runout scenarios provided by Allan (1931) and BGC Engineering Inc. (2000) that have been used for all discussions and planning for emergency response with the municipality and provincial emergency management officials are based on the assumption of one single large rock failure (Moreno and Froese, 2009a). These previous scenarios were made prior to the advances in mapping technologies and runout models that are available today. The current study indicates that the most active areas in terms of movement comprise many smaller volume rock masses, implying limited runout compared to a single large-volume failure. The maximum runout produced by modelling of limited-volume runouts has been compared with the runouts previously calculated for large, single-event scenarios (Figure 23); this information has been communicated formally to the municipality and provincial emergency-management officials. Although the visible signs of activity observed during field mapping indicate that a series of smaller volume failures is more likely to occur, the potential for a single large volume failure cannot be ignored. Based on this, the current planning for emergency response and evacuation continues to use the larger volume runout estimate provided by BGC Engineering (2000).

As the potentially unstable structures have only recently been identified and there was no information on the spatial and temporal characteristics of the deformation, the monitoring system has been extended to the lower Third Peak and lower South Peak areas to characterize the potential movements. This system consists of an array of overlapping global positioning system (GPS) monitoring points (both continuously and periodically monitored) and a series of twenty mirror prisms, which are monitored via a robotic total station from across the valley. Based on the results of monitoring from the EDM system (Moreno and Froese, 2009b), photogrammetric targets (Froese et al., 2009), dGPS (Moreno and Froese, 2009b) and the GB-InSAR (Dehls et al., 2010), movement rates of up to 5 mm/year have been observed on the active crown area. As there is good agreement between the various monitoring results, this indicates that these technologies are able to quantify very slow movements. This improves our confidence that the movements in other portions of the eastern face of the mountain are within detectable limits. The fact that no movements have been detected to date on these systems in other parts of the mountain indicates that any movements, if occurring, are less than a few millimetres per year.

7 References

Allan, J.A. (1931): Report on stability of Turtle Mountain, Crowsnest District, Alberta; Alberta Department of Public Works, Alberta Provincial Archives, 14 p.

AMEC Earth and Environmental (2005): Turtle Mountain monitoring project, summary report—WP 11.03 and 12.03, subsurface geotechnical and microseismic monitoring system; unpublished report prepared by AMEC Earth and Environmental for Alberta Municipal Affairs, 17 p.

Antonello, G., Casagli, N., Farina, P., Leva, D., Nico, G., Sieber, A.J. and Tarchi, D. (2004): Ground-based SAR interferometry for monitoring mass movements; Landslides, v. 1, no. 1, p. 21–28.

BGC Engineering Inc. (2000): Geotechnical hazard assessment of the south flank of Frank Slide, Hillcrest, Alberta; unpublished report prepared for Alberta Environment under Contract 00-0153, 29 p.

Bjorgan, G. (2010): Turtle Mountain monitoring, April repair trip report; unpublished report prepared by NavStar Geomatics Ltd for Alberta Geological Survey, 8 p.

Charriere, M. (2011): Granulometrical, geological and morphological description of the Frank Slide deposit (Alberta, Canada); M.Sc. thesis, University of Lausanne, 170 p.

Dade, W.B. and Huppert, H.E. (1998): Long-runout rockfalls; Geology, v. 26, p. 803–806.

Daly, R.A., Miller, W.G. and Rice, G.S. (1912): Report of the commission appointed to investigate Turtle Mountain, Frank, Alberta; Geological Survey of Canada, Memoir 27, 34 p.

Dehls, J.F., Giudici, D., Mariotti, F., Farina, P., Martin, D. and Froese, C.R. (2010): Monitoring Turtle Mountain using ground-based synthetic aperture radar (GB-InSAR); *in* Proceedings of the 63rd International Canadian Geotechnical Conference of the Canadian Geotechnical Society, Calgary, Alberta, 6 p.

Fraser, C.S. (1983): Deformation of Turtle Mountain by high precision photogrammetry; Alberta Environment Research Management Division, Report L0-83, 43 p.

Froese, C.R., Moreno, F., Jaboyedoff, M. and Cruden, D.M. (2009): 25 years of movement monitoring on the South Peak of Turtle Mountain: understanding the hazard; Canadian Geotechnical Journal, v. 46, p. 256–269.

Goguel, J. (1978): Scale-dependent rockslide mechanisms, with emphasis on the role of pore fluid vaporization; Rockslides and Avalanches, Natural Phenomena, Elsevier, Amsterdam, v. 1, p. 693–705.

Heim, A. (1932): Der Bergsturz und Menschenlenben; Fretz und Wasmuth Verlag, Zurich, 218 p.

Hsu, K.J. (1975): Catastrophic debris streams (strurzstroms) generated by rockfall; Geological Society of America Bulletin, v. 86, p. 129-140.

Hungr, O. (2008): Turtle Mountain, Frank, Alberta: run-out analyses of potential landslides on South and Third Peaks; unpublished report prepared for Alberta Geological Survey, 51 p.

Kent, P.E. (1966): The transport mechanism in catastrophic rock falls; Journal of Geology, v. 74, p. 79–83.

Laffin, R. (2010): Turtle Mountain monitoring, summer 2010 repair and upgrade; unpublished report prepared by Campbell Scientific for Alberta Geological Survey, 5 p.

Melosh, H.J. (1987): The mechanics of large rock avalanches; Geological Society of America, Review in Engineering Geology, v. 7, p. 41–49.

Moreno, F. and Froese C.R. (2006): Turtle Mountain Field Laboratory monitoring and research summary report, 2005; Alberta Energy and Utilities Board, EUB/AGS Earth Sciences Report 2006-07, 94 p., URL <http://www.ags.gov.ab.ca/publications/abstracts/ESR_2006_07.html> [May 2011].

Moreno, F. and Froese, C.R. (2008a): Turtle Mountain Field Laboratory: 2006 data and activity summary; Energy Resources Conservation Board, ERCB/AGS Open File Report 2008-1, 29 p., URL <http://www.ags.gov.ab.ca/publications/abstracts/OFR_2008_01.html> [May 2011].

Moreno, F. and Froese, C.R. (2008b): Turtle Mountain Field Laboratory: 2007 data and activity summary; Energy Resources Conservation Board, ERCB/AGS Open File Report 2008-7, 40 p., URL <http://www.ags.gov.ab.ca/publications/abstracts/OFR_2008_07.html> [May 2011].

Moreno, F. and Froese, C.R. (2009a): ERCB/AGS roles and responsibilities manual for the Turtle Mountain Monitoring Project, Alberta; Energy Resources Conservation Board, ERCB/AGS Open File Report 2009-06, 22 p., URL <http://www.ags.gov.ab.ca/publications/abstracts/OFR_2009_06.html> [May 2011].

Moreno, F. and Froese, C.R. (2009b): Turtle Mountain Field Laboratory: 2008 data and activity summary; Energy Resources Conservation Board, ERCB/AGS Open File Report 2009-15, 22 p., URL <http://www.ags.gov.ab.ca/publications/abstracts/OFR_2009_15.html> [May 2011].

Moreno, F. and Froese, C.R. (2011): Turtle Mountain Field Laboratory: 2009 data and activity summary; Energy Resources Conservation Board, ERCB/AGS Open File Report 2011-05, 22 p., URL <http://www.ags.gov.ab.ca/publications/abstracts/OFR_2011_05.html> [May 2011].

Pedrazzini, A. and Jaboyedoff, M. (2008): Turtle Mountain stability analysis project: morpho-structural analysis and estimation of the potential unstable volumes; unpublished report IGAR-AP-R003 prepared by the Institute of Geomatics and Risk Analysis, University of Lausanne for Alberta Geological Survey, 31 p.

Pedrazzini, A., Jaboyedoff, M., Froese, C.R, Langenberg, C.W. and Moreno, F. (2011): Structural analysis of Turtle Mountain, origin and influence of fractures in the development of rock failure; Slope Tectonics, special publication, Geological Society of London, v. 351, p. 163–183.

Pedrazzini, A., Jaboyedoff, M., Froese, C.R, Hungr, O. and Humair, F. (in press): Combining digital elevation model analysis and run-out modeling to characterize hazard posed by a potentially unstable rock slope at Turtle Mountain; Engineering Geology, available online 08-Apr-2011. doi:10.1016/j.enggeo.2011.03.015

Teskey, B. and Ebeling, A. (2010): Turtle Mountain deformation monitoring, 2007–2010, final report; unpublished report prepared by the Department of Geomatics Engineering, University of Calgary for Alberta Geological Survey, 21 p.